

# Causal Inference on Non-linear Spaces: Distribution Functions and Beyond

Zhenhua Lin<sup>1</sup>, Dehan Kong<sup>2</sup>, and Linbo Wang<sup>2</sup>

<sup>1</sup> National University of Singapore, Singapore

<sup>2</sup> University of Toronto, Toronto, Ontario, Canada

## Abstract

Understanding causal relationships is one of the most important goals of modern science. So far, the causal inference literature has focused almost exclusively on outcomes coming from a linear space, most commonly the Euclidean space. However, it is increasingly common that complex datasets collected through electronic sources, such as wearable devices and medical imaging, cannot be represented as data points from linear spaces. In this paper, we present a formal definition of causal effects for outcomes from non-linear spaces, with a focus on the Wasserstein space of cumulative distribution functions. We develop doubly robust estimators and associated asymptotic theory for these causal effects. Our framework extends to outcomes from certain Riemannian manifolds. As an illustration, we use our framework to quantify the causal effect of marriage on physical activity patterns using wearable device data collected through the National Health and Nutrition Examination Survey.

*Keywords:* Double robustness, Object oriented data analysis, Riemannian manifolds, Wasserstein space

# 1 Introduction

Causal inference has received increasing attention in contemporary data analysis. In many modern applications such as medical imaging, computer vision and bioinformatics, the observed data are sampled from non-linear spaces such as spheres, spaces of symmetric positive definite matrices, and space of images. So far, researchers in causal inference have engaged almost exclusively in studying causal effects on objects from a linear space, most commonly the Euclidean space  $\mathbb{R}^p$ . There are fundamental challenges in extending existing methods to study causal effects on outcomes defined on non-linear spaces. For example, a common measure of causal influence is the average causal effect, defined as the difference between the expectations of potential outcomes under different treatment values. However, neither the expectations nor the difference is well-defined if the potential outcomes come from a non-linear space.

One of the most common non-linear spaces in statistics consists of probability measures on a real interval  $\mathcal{I}$ . This space is commonly equipped with a so-called Wasserstein distance based on the geometry of optimal transportation, and then referred to as the Wasserstein space. The Wasserstein space is clearly non-linear as linear combinations of probability distributions may not be a probability distribution. There has been extensive literature studying causal effects on a summary measure of the probability distribution, most commonly the mean or quantiles. However, in many occasions, ideally practitioners would like to know the causal effect on the distributions themselves, thereby circumventing the need to come up with a, often subjective, summary measure of the distributions.

**Example 1** (Physical activity patterns). *Behavioral scientists are often interested in evaluating the effects of potential risk factors, such as marriage, on physical activity patterns (e.g. King et al., 1998). The physical activity patterns are often recorded over a certain monitoring period. For example, in the National Health and Nutrition Examination Survey 2005–2006, physical activity intensity, ranging from 0 to 32767 counts per minute (cpm), was recorded consecutively for 7 days by a wearable device for subjects at least six years old. The trajectory of activity intensity, denoted by the function  $Z(t)$ , is not directly comparable across different subjects as different individuals might have different circadian rhythms. Instead, the distribution of activity intensity is invariant to circadian rhythms and hence can be compared between groups of individuals. Specifically, let  $Y = \lambda(\{t : Z(t) \leq s\})/7$  be the distribution of physical activity intensity over 7 days, where  $\lambda$  denotes the Lebesgue measure.  $Y$  is a cumulative distribution function and belongs to the Wasserstein space  $\mathcal{W}_2(\mathcal{I})$  with  $\mathcal{I} = [0, 32767]$ , endowed with the distance  $d(F, G) = [\int \{F^{-1}(s) - G^{-1}(s)\}^2 ds]^{1/2}$ ; here  $F^{-1}(s)$  refers to the quantile function.*

The increasing availability of data residing in a Wasserstein space is accompanied by the

emerging field of statistical optimal transport. Among others, Aguech and Carlier (2011); Bigot et al. (2012); Kim and Pass (2017) studied theoretical properties of the Wasserstein barycenter, a generalization of the notion of averages in Euclidean spaces; Bigot et al. (2017) studied principal component analysis for data sampled from a Wasserstein space; Petersen and Müller (2016); Zhang et al. (2020) studied regression models for such data. For more related works on statistical data analysis in a Wasserstein space, we refer readers to the survey paper by Bigot (2020) and references therein.

Wasserstein spaces have a formal Riemannian structure (Ambrosio et al., 2004). Thus probability distributions residing in Wasserstein spaces may also be analyzed from the perspective of Riemannian geometric statistics. There is a vast literature for statistical analysis on Riemannian manifolds. Among others, Bhattacharya and Patrangenaru (2003, 2005); Schötz (2019); Eltzner and Huckemann (2019) studied properties of the Fréchet mean, which generalizes the concept of expectation from the Euclidean space to the Riemannian manifold; Yuan et al. (2012); Fletcher (2013); Cornea et al. (2017); Petersen and Müller (2019) studied regression problems on the Riemannian manifold or a general metric space. The monograph Patrangenaru and Ellingson (2015) provides a relatively comprehensive treatment on nonparametric statistics for Riemannian manifolds.

There is, however, a paucity of literature for causal inference on non-linear spaces, such as the Wasserstein space, or a general Riemannian manifold. Due to the curved geometry of the outcome space, extension of the traditional notion of average causal effect in the Euclidean space is non-trivial. Although the notion of Wasserstein barycenter (or Fréchet mean) can be used to generalize the notion of expectation, it is still challenging to define a contrast between Wasserstein barycenters so that it is both practically meaningful and statistically estimable.

The contributions of this paper are at least four-fold. First, building on the notion of optimal transport maps between probability distributions, we propose a novel definition of causal effects for distribution-valued outcomes, called the average causal effect map. Second, motivated by the similar Riemannian structures of the Wasserstein space  $\mathcal{W}_2(\mathcal{I})$  and Riemannian manifolds, we extend the notion of average causal effect map to Riemannian manifold-valued outcomes. To the best of our knowledge, this is the first systematic study on causal inference for distribution-valued or manifold-valued outcomes. Third, we show identifiability of the average causal effect map under standard assumptions in the causal inference literature, and develop doubly robust estimating procedures for the average causal effect map. Fourth, we establish the asymptotic properties of the proposed doubly robust estimators. In contrast to the setting for the classical doubly robust estimator (Robins et al., 1994; Vermeulen and Vansteelandt, 2015), typically even for a fixed individual, the outcome may not be fully observed and needs to be estimated from

data. For instance, in Example 1, one only observes the empirical distribution function rather than the true distribution function for each individual. To establish the asymptotic properties with distribution-valued outcomes, our analyses rely on several geometric properties of the Wasserstein space, most notably the isometry between the Wasserstein space and the space of quantile functions. When the outcomes come from a general Riemannian manifold, our asymptotic analyses rely on a Riemannian generalization of Taylor expansion, which was traditionally used outside of the statistical literature. Unlike the Euclidean or Wasserstein spaces which are “flat”, our analysis reveals that the curvature of the underlying Riemannian manifold contributes an additional term to the asymptotic variance of the proposed doubly robust estimator; see Theorem 5(ii) for details.

The rest of the paper is structured as follows. In Section 2, we present background on causal inference, Wasserstein space and Riemannian manifolds. In Section 3 we introduce the notion of average causal effect map for outcomes from a Wasserstein space, develop identifiability results and estimators for the average causal effect map, and study their asymptotic properties. We then generalize the average causal effect map and related estimators to accommodate Riemannian manifold-valued outcomes in Section 4. We provide numerical studies in Section 5 and a real data illustration in Section 6. We end with a brief discussion in Section 7.

## 2 Background

### 2.1 The potential outcomes framework

We define causal effects using the potential outcomes framework. Suppose that the treatment is  $A \in \{0, 1\}$ , with 0 and 1 being the labels for control and active treatments, respectively. We use  $X$  to denote baseline covariates taking values in  $\mathbb{R}^d$ . For each level of treatment  $a$ , we assume there exists a potential outcome  $Y(a)$ , representing the outcome had the subject, possibly contrary to the fact, been given treatment  $a$ . Here  $Y(a)$  is a random object that resides in a possibly non-linear space. We make the stable unit treatment unit assumption (SUTVA, Rubin, 1980) so that the potential outcomes for any unit do not vary with the treatments assigned to other units; for each unit, there are no different versions of treatments that lead to different potential outcomes. Under this assumption, the observed outcome  $Y = Y(A)$ , where  $Y(A) = Y(1)$  if  $A = 1$  and  $Y(A) = Y(0)$  if  $A = 0$ . We assume we observe  $n$  independent samples from an infinite super-population of  $(A, X, Y)$ , denoted as  $(A_i, X_i, Y_i), i = 1, \dots, n$ .

When  $Y(a)$  resides in  $\mathbb{R}$ , the causal effect is commonly defined as the contrast between a summary measure of the potential outcome distributions. For example, the average causal effect

is defined as the difference between the means of the potential outcome distributions:

$$\text{ACE} = \mathbb{E}\{Y(1)\} - \mathbb{E}\{Y(0)\}; \quad (1)$$

the quantile treatment effect is defined as the difference between the quantiles of the potential outcomes distributions

$$\text{QTE}(\alpha) = F_{Y(1)}^{-1}(\alpha) - F_{Y(0)}^{-1}(\alpha), \alpha \in [0, 1], \quad (2)$$

where  $F_Z(z) = P(Z \leq z)$  is the cumulative distribution function (CDF) of the random variable  $Z$  and  $F_Z^{-1}(\alpha) = \inf\{z : F_Z(z) \geq \alpha\}$  is the corresponding quantile function. Causal effects defined in this manner can be interpreted on the population level, as they concern contrasts between potential outcomes in two hypothetical populations. These population-level interpretations concern the effect of introducing a particular treatment to a population, and are most relevant to policy makers.

There is however, a subtle but important distinction between the individual-level interpretations of ACE and  $\text{QTE}(\alpha)$ . Let  $CE_i = Y_i(1) - Y_i(0)$  be the individual causal effect for unit  $i$ . Individual causal effects provide useful information for individualized treatment decision making, and are most relevant to individual subjects. Since  $\text{ACE} = \mathbb{E}(CE_i)$ , it can be interpreted as averages of individual causal effects; here the expectation is taken over units in the super-population. The individual-level interpretation of ACE extends to the conditional average treatment effect,  $\text{CACE}(L) = \mathbb{E}\{Y(1)|L\} - \mathbb{E}\{Y(0)|L\}$ , where  $L$  is a subset of observed baseline covariates. In contrast, generally  $\text{QTE}(\alpha)$  cannot be interpreted as the  $\alpha$ -quantile of individual causal effects.

## 2.2 Causal effect identification and estimation

The following assumptions are standard in the causal inference literature.

**Assumption 1** (Ignorability).  $A \perp\!\!\!\perp Y(a) | X, a = 0, 1$ .

**Assumption 2** (Positivity). *The propensity score  $\pi(X) := P(A = 1 | X)$  is bounded away from 0: there exists  $\epsilon > 0$ , such that  $\epsilon < \pi(X) < 1 - \epsilon$ , a.e..*

Under Assumptions 1 and 2, when  $Y(a)$  resides in  $\mathbb{R}$ , the mean potential outcome is given by

$$\mu_a := \mathbb{E}[Y(a)] = \mathbb{E}_X\{\mathbb{E}[Y | A = a, X]\} = \mathbb{E}\left\{\frac{I(A = a)Y}{P(A = a | X)}\right\}. \quad (3)$$

Similarly, the potential outcome distributions  $F_{Y(a)}(y)$  can be identified by replacing  $Y$  in the last term of eqn. (3) with  $I(Y \leq y)$ . Based on (3), the average causal effect can be identified as  $\text{ACE} = \mathbb{E}\{Y(1)\} - \mathbb{E}\{Y(0)\}$ , and the quantile treatment effect can be identified as  $\text{QTE}(\alpha) = F_{Y(1)}^{-1}(\alpha) - F_{Y(0)}^{-1}(\alpha)$ .

Given the identification formula (3), one may use plug-in estimators to estimate the mean potential outcomes. Let  $m_a(X) = \mathbb{E}(Y | A = a, X)$  and  $f(A | X) = A\pi(X) + (1 - A)(1 - \pi(X))$ . Also denote  $\hat{m}_a(X)$ ,  $\hat{\pi}(X)$ ,  $\hat{f}(A | X)$  as estimates of their corresponding population quantities obtained using standard parametric or nonparametric techniques. Some leading estimators of  $\mu_a$  include the outcome regression estimator  $\hat{\mu}_a^{OR} = \mathbb{P}_n \hat{m}_a(X)$ , the inverse probability weighting estimator  $\hat{\mu}_a^{IPW} = \mathbb{P}_n \frac{I(A = a)Y}{\hat{f}(A | X)}$ , and the so-called doubly robust estimator  $\hat{\mu}_a^{DR} = \hat{\mu}_a^{OR} + \mathbb{P}_n \left[ \frac{I(A = a)}{\hat{f}(A | X)} \{Y - \hat{m}_a(X)\} \right]$ ; here  $\mathbb{P}_n$  refers to the empirical average operator:  $\mathbb{P}_n(O) = \frac{1}{n} \sum_{i=1}^n O_i$ .

## 2.3 Wasserstein space

Let  $\mathcal{I}$  be an interval of  $\mathbb{R}$ ,  $V_1$  and  $V_2$  be random variables taking values in  $\mathcal{I}$  with finite second moments, and  $\lambda_1, \lambda_2$  be their (cumulative) distribution functions, respectively. To define the Wasserstein distance between  $\lambda_1$  and  $\lambda_2$ , we let  $\Lambda(\lambda_1, \lambda_2)$  denote all joint distributions  $\lambda_{12}$  of  $(V_1, V_2)$  that have marginal distributions  $\lambda_1$  and  $\lambda_2$ . The (2-)Wasserstein distance between  $\lambda_1$  and  $\lambda_2$  is defined as

$$W_2(\lambda_1, \lambda_2) = \left( \inf_{\lambda_{12} \in \Lambda(\lambda_1, \lambda_2)} \int_{\mathcal{I} \times \mathcal{I}} (s - t)^2 d\lambda_{12}(s, t) \right)^{1/2}. \quad (4)$$

The Wasserstein space of order 2 on  $\mathcal{I}$  is then defined as the space of distribution functions on  $\mathcal{I}$  with finite second moments

$$\mathcal{W}_2(\mathcal{I}) = \left\{ \lambda \text{ is a distribution function on } \mathcal{I} : \int_{\mathcal{I}} t^2 d\lambda(t) < \infty \right\}$$

endowed with the 2-Wasserstein distance.

The Wasserstein distance can be motivated by the problem of optimal transport. Consider a pile of mass on space  $\mathcal{I}$  with a distribution  $\lambda_1$ . We wish to transport the mass in such a way that the new mass distribution is  $\lambda_2$ . Assume also that the cost of transporting a unit mass from point  $s$  to point  $t$  is  $(s - t)^2$ . A transport plan to move  $\lambda_1$  to  $\lambda_2$  can be described by the function  $\lambda_{12}$  such that  $d\lambda_{12}(s, t)$  denotes the amount of mass to move from  $s$  to  $t$ . Since the amount of mass to be moved out of  $s$  must match  $d\lambda_1(s)$ , and the amount of mass to be moved into  $t$  must match  $d\lambda_2(t)$ , we have  $\int_{t \in \mathcal{I}} d\lambda_{12}(s, t) = d\lambda_1(s)$ ,  $\int_{s \in \mathcal{I}} d\lambda_{12}(s, t) = d\lambda_2(t)$ . In

other words,  $\lambda_{12} \in \Lambda(\lambda_1, \lambda_2)$ . The Wasserstein distance then corresponds to the minimum effort that is required in order to transport the mass of  $\lambda_1$  to produce the mass distribution of  $\lambda_2$ . The minimizer  $\lambda_{12}^*$  to the problem in (4) always exists (Santambrogio, 2015, Theorems 1.7 and 1.22) and is known as the optimal transport plan.

If  $\lambda_1$  is continuous, then there exists a unique function  $T(\cdot) : \mathcal{I} \rightarrow \mathcal{I}$  such that  $d\lambda_{12}^*(s, T(s)) = d\lambda_1(s)$  (Santambrogio, 2015, Theorems 1.7 & 1.22). Intuitively, in this case, the optimal transport plan moves all the mass at  $s$  to  $T(s)$ . The function  $T(\cdot)$  is known as the optimal transport map. Let  $\lambda^{-1}$  be the quantile function of the distribution  $\lambda$ . It can be shown that (Ambrosio et al., 2005, Theorem 6.0.2) the optimal transport map  $T(s) = \lambda_2^{-1}(\lambda_1(s))$ , so that it moves mass between corresponding quantiles of  $\lambda_1$  and  $\lambda_2$ . The following proposition, summarizing the above discussion, shows that given a fixed continuous distribution  $\lambda_1$ , the distribution  $\lambda_2$  can be defined via the optimal transport map from  $\lambda_1$  to  $\lambda_2$ . The proof of Proposition 1 is straightforward and hence omitted.

**Proposition 1.** *Given a continuous distribution function  $\lambda_1$ , there is a one-to-one correspondence between a distribution function  $\lambda_2$  and the optimal transport map from  $\lambda_1$  to  $\lambda_2$ .*

Based on the notion of Wasserstein distance  $W_2$ , we can define the mean of a set of distributions  $\lambda_1, \dots, \lambda_n$  in the Wasserstein space by the so-called Wasserstein barycenter  $\bar{\lambda}$ , defined as the distribution  $\lambda$  that minimizes  $\frac{1}{n} \sum_{i=1}^n W_2^2(\lambda_i, \lambda)$ . In Lemma 2 in the Supplementary Material, it is shown that  $\bar{\lambda}^{-1} = \frac{1}{n} \sum_{i=1}^n \lambda_i^{-1}$ , so that the quantile function corresponding to the Wasserstein barycenter equals the (Euclidean) averages of the individual quantile functions. The mean of distributions can also be defined in various other ways, such as the mean under the Euclidean distance  $\frac{1}{n} \sum_{i=1}^n \lambda_i$ . Compared to alternative center measures, the Wasserstein barycenter typically provides a better summary that captures the structure of the random objects represented by distribution functions, such as shapes, curves, and images; see for example, Cuturi and Doucet (2014, Figure 1) for an illustration.

## 2.4 Riemannian manifolds

Key notions in the Wasserstein space, in particular Proposition 1, extend to other metric spaces such as connected Riemannian manifolds. A formal presentation of these extensions requires heavy technicalities from differential geometry and thus is deferred to the Supplementary Material. Here we provide a brief introduction to related concepts at a high level.

Recall from basic topology that one can define continuous functions between topological spaces. For an interval  $I \subset \mathbb{R}$  containing 0, a curve  $\gamma : I \rightarrow \mathcal{M}$  is a continuous function mapping

$I$  into a topological space  $\mathcal{M}$ . To define derivatives for  $\gamma$ , we shall equip  $\mathcal{M}$  with additional structures so that it becomes a differentiable manifold. This can be completed in two steps. First, we say a topological space is a *(topological) manifold* if it locally resembles a linear space near each point. In particular, a manifold  $\mathcal{M}$  modeled on  $\mathbb{R}^q$  is a topological space so that at each point on  $\mathcal{M}$  there is a neighborhood that is homeomorphic to  $\mathbb{R}^q$ , where a homeomorphism is a continuous and one-to-one mapping whose inverse is also continuous. We can define  $\gamma'(0)$  via a local homeomorphism to a Euclidean space at  $\gamma(0)$ ; see the Supplementary Material for a detailed definition. Note that different homeomorphisms at  $\gamma(0)$  may lead to different versions of  $\gamma'(0)$ . Second, a *differential manifold* is a type of manifold with a globally defined differential structure. Informally, it requires the homeomorphisms at different neighborhoods are compatible with each other in the sense that there is a differentiable transition between them. If the transition is infinitely differentiable, or smooth, then we say the manifold is smooth.

As an example, consider the unit sphere  $\mathbb{S}^2 = \{(x_1, x_2, x_3) \in \mathbb{R}^3 : x_1^2 + x_2^2 + x_3^2 = 1\}$ . Let  $U_1 = \mathbb{S}^2 \setminus \{(1, 0, 0)\}$  and  $U_2 = \mathbb{S}^2 \setminus \{(-1, 0, 0)\}$ . Although there is no homeomorphism between  $\mathbb{S}^2$  and  $\mathbb{R}^2$ , there is a homeomorphism between  $U_i, i = 1, 2$  and  $\mathbb{R}^2$ . Since for each point  $\lambda$  on  $\mathbb{S}^2$ , there is at least one of  $U_i, i = 1, 2$  such that it is a neighborhood of  $\lambda$ ,  $\mathbb{S}^2$  is a manifold modeled on  $\mathbb{R}^2$ . As discussed in detail in the Supplementary Material,  $\mathbb{S}^2$  is in fact a smooth manifold.

Based on the notion of derivatives, we now introduce tangent spaces for a differential manifold  $\mathcal{M}$ . For each point  $\lambda \in \mathcal{M}$ , we say two curves  $\gamma_1$  and  $\gamma_2$  are equivalent at  $\lambda$  if  $\gamma_1(0) = \gamma_2(0) = \lambda$  and  $\gamma_1'(0) = \gamma_2'(0)$ . An equivalence class of curves at  $\lambda$  is called a tangent vector at  $\lambda$ , and the collection of the tangent vectors at  $\lambda$  is called the *tangent space* at  $\lambda$ , conveniently denoted by  $T_\lambda \mathcal{M}$ . It can be shown that the definition of tangent vector is intrinsic in the sense that it does not depend on the specific choice of the homeomorphism at  $\gamma(0)$ . When endowed with a vector structure, a tangent space becomes a linear space. In fact, the tangent space may sometimes be visualized as a hyperplane in a Euclidean space. For example, the tangent space at point  $\lambda \in \mathbb{S}^2$  can be visualized as the tangent plane at that point, that is  $T_\lambda \mathbb{S}^2 = \{v \in \mathbb{R}^3 : v \cdot \lambda = 0\}$ , where  $\cdot$  denotes the dot product on  $\mathbb{R}^3$ ; see Figure S2 in the Supplementary Material for an illustration.

A Riemannian manifold  $\mathcal{M}$  is then defined as a real, smooth manifold equipped with an inner product  $g_\lambda$  on the tangent space  $T_\lambda \mathcal{M}$  at each point  $\lambda$  that varies smoothly from point to point. If  $\mathcal{M}$  is also connected, then  $g_\lambda$  collectively induce a unique distance function  $d$  on  $\mathcal{M}$  so that it becomes a metric space. If  $\mathcal{M}$  is furthermore complete, then by the Hopf-Rinow theorem, we can “project” any vector in the tangent space  $T_\lambda \mathcal{M}$  to a point in  $\mathcal{M}$ , known as the Riemannian exponential map  $\mathcal{E}_\lambda$ . When  $\mathcal{E}_\lambda$  is invertible, its inverse, denoted as the Riemannian logarithmic map  $\mathcal{L}_\lambda$ , maps an element in  $\mathcal{M}$  to a vector in  $T_\lambda \mathcal{M}$ ; see Figure S2

in the Supplementary Material for an illustration.

We conclude this section with a note that the Wasserstein space  $\mathcal{W}_2(\mathcal{I})$  is not a Riemannian manifold (Bigot et al., 2017). However, as we discuss later in Interpretation 4, it can be endowed with a Riemannian structure including the tangent space and Riemannian logarithmic map. These similarities between the two spaces allow us to extend the proposed definition of causal effect from random distributions to random elements residing on a Riemannian manifold.

## 3 Causal Inference on Distribution Functions

### 3.1 Definition of causal effects

We now introduce a definition of average causal effect for outcomes taking value in the Wasserstein space  $\mathcal{W}_2(\mathcal{I})$ . In parallel to the definition of causal effects introduced in Section 2.1, we first define the mean potential outcomes. As both  $Y_i(1)$  and  $Y_i(0)$  take value in the Wasserstein space, we define their means using their Wasserstein barycenters:

$$\mu_a = \mathbb{E}Y(a) \equiv \arg \min_{v \in \mathcal{W}_2(\mathcal{I})} \mathbb{E} \left\{ W_2^2(Y(a), v) \right\}, \quad a = 0, 1. \quad (5)$$

Intuitively,  $\mu_a$  is a “typical” potential distribution under treatment  $A = a$ . Let  $\delta_t$  denote the Dirac delta function with point mass at  $t$ . Ideally a causal effect definition in the Wasserstein space should satisfy the following desiderata:

- (a) In the degenerate case where  $Y_i(a) = \delta_{y_i(a)}$ , corresponding to the classical scenario where the outcome resides in  $\mathbb{R}$ , the causal effect corresponds to the usual average causal effect ACE defined in (1);
- (b) When  $\mathbb{E}Y(1) = \mathbb{E}Y(0)$ , the causal effect equals zero;
- (c) The average causal effect is a contrast between the averages of potential outcomes in two hypothetical populations,  $Y(1)$  and  $Y(0)$ , and thus can be interpreted on the population level;
- (d) The average causal effect equals the average of individual causal effects, thus maintaining the individual-level interpretation of the usual ACE discussed at the end of Section 2.1.

Naively, it may be tempting to define the causal effect as the Wasserstein distance between  $\mu_1$  and  $\mu_0$ . However, although it satisfies desiderata (a) - (c), in general desideratum (d) fails to hold. Instead, we introduce a novel definition of average causal effect, called the *causal effect*

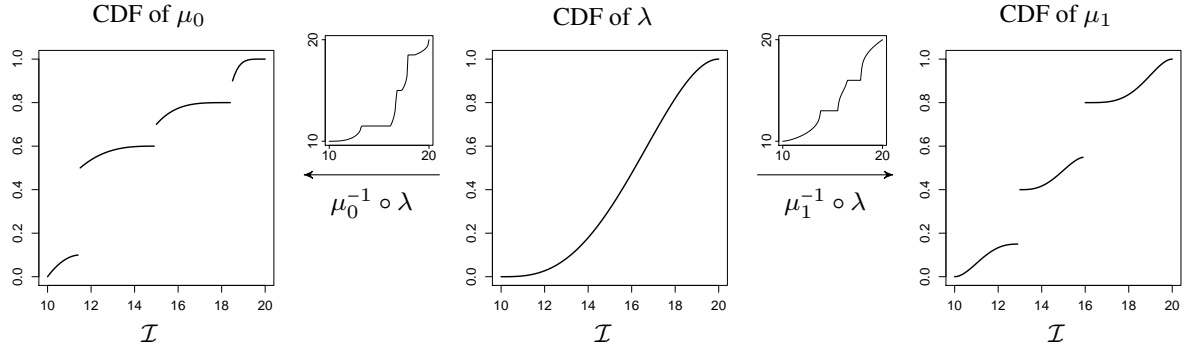


Figure 1: Illustration of the causal effect map between two mixed distributions  $\mu_1$  and  $\mu_0$  on  $\mathcal{I} = [10, 20]$  with respect to a common continuous reference distribution  $\lambda$ .

*map.* We shall see that the causal effect map satisfies all the desiderata, and contains richer information than the single summary measure  $W_2(\mu_1, \mu_0)$  in the sense that one can compute  $W_2(\mu_1, \mu_0)$  based on the causal effect map.

**Definition 1.** Let  $\lambda$  be a continuous distribution function in  $\mathcal{W}_2(\mathcal{I})$ . The individual causal effect map of  $A$  on  $Y$  is defined as

$$\Delta_i^\lambda(\cdot) = Y_i(1)^{-1} \circ \lambda(\cdot) - Y_i(0)^{-1} \circ \lambda(\cdot), \quad (6)$$

where we say  $\lambda$  is a reference distribution. The (average) causal effect map of  $A$  on  $Y$  is defined as

$$\Delta^\lambda(\cdot) = (\mathbb{E} Y(1))^{-1} \circ \lambda(\cdot) - (\mathbb{E} Y(0))^{-1} \circ \lambda(\cdot) = (\mu_1^{-1} - \mu_0^{-1}) \circ \lambda(\cdot). \quad (7)$$

All causal effect maps are contrasts between two mappings from  $\mathcal{I}$  to  $\mathcal{I}$ .

**Interpretation 1** (Optimal transport from a common reference distribution). Motivated by Proposition 1, in (6) and (7), we define the contrast between two distribution functions by comparing them to a continuous reference distribution  $\lambda$ . For example, as illustrated in Figure 1, the average causal effect map is defined as the difference between the optimal transport maps from the reference distribution  $\lambda$  to the Wasserstein barycenters under two hypothetical distributions,  $\mu_1$  and  $\mu_0$ . Note that only the reference distribution  $\lambda$  needs to be continuous, while the barycenters  $\mu_1$  and  $\mu_0$  may be any element in the Wasserstein space  $\mathcal{W}_2(\mathcal{I})$ .

It is easy to verify that for any choice of reference distribution  $\lambda$ , the causal effect map satisfies desiderata (a) - (c). The following Theorem 1 shows that it also satisfies desideratum (d).

**Theorem 1.** *The average causal effect map corresponds to the average of individual causal effect maps with respect to the same reference distribution  $\lambda$ :*

$$\Delta^\lambda(\cdot) = \mathbb{E}\Delta_i^\lambda(\cdot) = \mathbb{E}\{Y(1)^{-1} \circ \lambda(\cdot) - Y(0)^{-1} \circ \lambda(\cdot)\}.$$

Theorem 1 can be proved using Lemma 2 in the Supplementary Material. As we will see later in Section 3.2, Theorem 1 is crucial for identification of the average causal effect map.

The following proposition shows that one may compute the Wasserstein distance  $W_2(\mu_1, \mu_0)$  from the causal effect map  $\Delta^\lambda(\cdot)$ . In particular, for any  $U$  that follows the reference distribution  $\lambda$ ,  $W_2(\mu_1, \mu_0)$  equals the  $\ell_2$ -norm of  $\Delta^\lambda(U)$ . It can be proved using Lemma 1 in the Supplementary Material.

**Proposition 2.** *The Wasserstein distance  $W_2(\mu_1, \mu_0)$  is determined by the causal effect map  $\Delta^\lambda(\cdot)$  via*

$$W_2(\mu_1, \mu_0) = \|\Delta^\lambda\|_\lambda := \left\{ \mathbb{E}_{U \sim \lambda} (\Delta^\lambda)^2(U) \right\}^{1/2} = \left\{ \int (\Delta^\lambda)^2(u) d\lambda(u) \right\}^{1/2}.$$

Desiderata (a) - (d) and Proposition 2 hold for any choice of the reference distribution  $\lambda$ . Our next result shows that when the potential outcomes  $Y(1), Y(0)$ , and hence the barycenters  $\mu_1$  and  $\mu_0$  (e.g. Bigot et al., 2017, Proposition 4.1), are continuous distributions, certain choices of the reference distribution lead to an alternative interpretation of the causal effect maps.

**Interpretation 2** (Optimal transports between continuous potential outcomes). *Consider the case where the potential outcomes are random continuous distribution functions. In this case, the optimal transport maps between the potential outcomes are of natural interest, including the individual causal transport map  $T_i(\cdot) = Y_i(1)^{-1} \circ Y_i(0)(\cdot)$  and the (population) causal transport map  $T(\cdot) = \mu_1^{-1} \circ \mu_0(\cdot)$ . The following proposition shows that under certain reference distributions, the causal effect maps are connected to the causal transport maps. It can be proved by replacing  $\lambda$  in (7) (resp. (6)) with  $\mu_0$  or  $\mu_1$  (resp.  $Y_i(0)$  or  $Y_i(1)$ ).*

**Proposition 3.** *If the potential outcomes are continuous distribution functions, then*

$$\begin{aligned} \Delta^{\mu_0} &= T - \text{id} = \mu_1^{-1} \circ \mu_0 - \text{id} \quad \text{and} \quad \Delta_i^{Y_i(0)} = T_i - \text{id} = Y_i(1)^{-1} \circ Y_i(0) - \text{id}; \\ \Delta^{\mu_1} &= \text{id} - T^{-1} = \text{id} - \mu_0^{-1} \circ \mu_1 \quad \text{and} \quad \Delta_i^{Y_i(1)} = \text{id} - T_i^{-1} = \text{id} - Y_i(0)^{-1} \circ Y_i(1), \end{aligned} \tag{8}$$

where  $\text{id}$  is the identity function.

In contrast to Theorem 1, the population causal transport map is generally different from the average of individual causal transport maps:  $T \neq \mathbb{E}[T_i]$ . To see this, note that due to

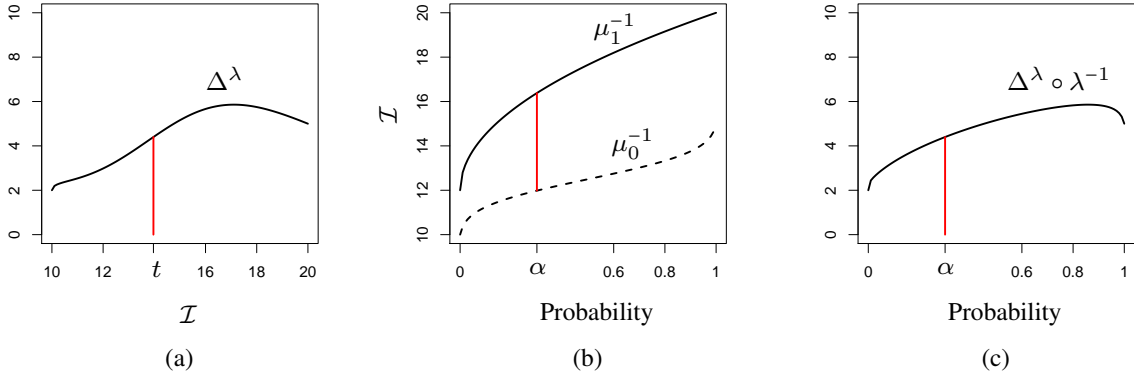


Figure 2: Interpreting the causal effect map as difference in quantiles: an illustration with  $\mathcal{I} = [10, 20]$ . The value  $\Delta^\lambda(t)$  at  $t$ , highlighted in red on panel (a), coincides with the difference (highlighted in red panel (b)) between  $\mu_1^{-1}(\alpha)$  and  $\mu_0^{-1}(\alpha)$  for  $\alpha = \lambda(t)$ . Panel (c) shows the causal effect map after a monotone transform of the input variable:  $\Delta^\lambda \circ \lambda^{-1}(\alpha) = \mu_1^{-1}(\alpha) - \mu_0^{-1}(\alpha)$ . The curves in (a) and (c) would agree exactly if the reference distribution  $\lambda$  equal the uniform distribution on  $\mathcal{I}$ .

eqn. (8),  $T = \Delta^{\mu_0} + \text{id}$ , while  $T_i = \Delta_i^{Y_i(0)} + \text{id}$ . Although as we show in Theorem 1, under the same reference distribution  $\lambda$ ,  $\Delta^\lambda = \mathbb{E}\Delta_i^\lambda$ , in general,  $\Delta^{\mu_0} \neq \mathbb{E}\Delta_i^{Y_i(0)}$ . As we illustrate later in Section 6, Proposition 3 provides guidance for estimating the causal transport map for a particular individual  $i$ . Instead of estimating the population causal transport map, one first estimates the individual causal effect map for individual  $i$  using the average causal effect map with reference distribution  $Y_i = Y_i(A_i)$ , and then use (8) to obtain an estimate of  $T_i(\cdot)$ .

**Interpretation 3** (Difference in quantiles). *The causal effect map  $\Delta(\cdot)$  can also be interpreted as difference in quantiles after a monotone transform of the input variable using the reference distribution. As we illustrate in Figure 2, if the interval  $\mathcal{I} = [10, 20]$ ,  $\Delta^\lambda(\cdot)$  is a mapping from  $[10, 20]$  to  $[-10, 10]$ . By definition, for  $t \in [10, 20]$ ,  $\Delta^\lambda(t) = \mu_1^{-1}(\alpha) - \mu_0^{-1}(\alpha)$ , where  $\alpha = \lambda(t)$ . Hence  $\Delta^\lambda(t)$  can be interpreted as the difference between the  $\alpha$ -quantiles of the mean potential outcomes under treatment and control, respectively. In this sense, the choice of reference distribution  $\lambda$  is nuisance to the interpretation of the causal effect map.*

The interpretation in terms of difference in quantiles is not to be confused with the quantile treatment effect defined in (2). In our setting, the potential outcomes are random distribution functions, and  $\mu_1^{-1}(\alpha)$  is the  $\alpha$ -quantile of *the mean potential outcome* under treatment. In contrast, in the quantile treatment effect setting, the realizations of potential outcomes are real numbers, and  $F_{Y(1)}^{-1}(\alpha)$  is the  $\alpha$ -quantile of *the distribution of potential outcomes* under treatment.

**Interpretation 4** (Projection to a tangent space). *For a continuous reference distribution  $\lambda$ , consider the space*

$$T_\lambda \mathcal{W}_2(\mathcal{I}) = \text{cl}\{k(v^{-1} \circ \lambda - \text{id}) : v \in \mathcal{W}_2(\mathcal{I}), k \in \mathbb{R}^+\},$$

where  $\text{cl}(S)$  denotes the closure of set  $S$ . It can be shown that  $T_\lambda \mathcal{W}_2(\mathcal{I})$  is a linear subspace of  $L^2(\mathcal{I}; \lambda) = \{h \in \mathbb{R}^\mathcal{I} : \int_{\mathcal{I}} |h|^2 d\lambda < \infty\}$  endowed with the inner product  $\langle h_1, h_2 \rangle_\lambda = \int_{\mathcal{I}} h_1 h_2 d\lambda$  and the induced norm  $\|h\|_\lambda = \langle h, h \rangle_\lambda^{1/2}$ .  $T_\lambda \mathcal{W}_2(\mathcal{I})$  can be viewed as the tangent space of  $\mathcal{W}_2(\mathcal{I})$  at  $\lambda$ , and for a fixed  $\lambda \in \mathcal{W}_2(\mathcal{I})$ , the mapping  $h \mapsto \lambda \circ (h + \text{id})^{-1}$  that maps an element on  $T_\lambda \mathcal{W}_2(\mathcal{I})$  to  $\mathcal{W}_2(\mathcal{I})$ , can be viewed as the Riemannian exponential map at  $\lambda$  (Ambrosio et al., 2004). Its inverse  $v \mapsto v^{-1} \circ \lambda - \text{id} := \mathcal{L}_\lambda v - \text{id}$  is the corresponding Riemannian logarithmic map at  $\lambda$ . From this perspective, the individual causal effect maps can be written as

$$\Delta_i^\lambda = \mathcal{L}_\lambda Y_i(1) - \mathcal{L}_\lambda Y_i(0) = \{\mathcal{L}_\lambda Y_i(1) - \text{id}\} - \{\mathcal{L}_\lambda Y_i(0) - \text{id}\}, \quad (9)$$

so they may be equivalently defined as the contrasts between the Riemannian logarithmic maps of distribution functions  $Y_i(1), Y_i(0)$ . By Theorem 1, the average causal effect map may then be equivalently defined as  $\Delta^\lambda = \mathbb{E}(\mathcal{L}_\lambda Y(1) - \text{id}) - \mathbb{E}(\mathcal{L}_\lambda Y(0) - \text{id})$ .

### 3.2 Identification and estimation

Under the ignorability and positivity assumptions, similar to Proposition (3), we can identify the causal effect map  $\Delta^\lambda$ .

**Theorem 2.** *Under Assumptions 1 and 2, for  $a = 0, 1$ , the average causal effect map  $\Delta^\lambda$  is identifiable and is given by*

$$\Delta^\lambda = \sum_{a=0,1} (2a-1) \mathbb{E}_X \{ \mathbb{E}[(Y^{-1} \circ \lambda) | A = a, X] \} = \sum_{a=0,1} (2a-1) \mathbb{E} \left\{ \frac{I(A = a)(Y^{-1} \circ \lambda)}{P(A = a | X)} \right\}. \quad (10)$$

To see the first equality in (10), note that

$$\begin{aligned} \Delta^\lambda &= \sum_{a=0,1} (2a-1) \mathbb{E} \{ Y(a)^{-1} \circ \lambda \} \quad (\text{due to Theorem 1}) \\ &= \sum_{a=0,1} (2a-1) \mathbb{E}_X [\mathbb{E}\{Y(a)^{-1} \circ \lambda | A = a, X\}] \quad (\text{due to ignorability}) \\ &= \sum_{a=0,1} (2a-1) \mathbb{E}_X [\mathbb{E}\{Y^{-1} \circ \lambda | A = a, X\}] \quad (\text{due to the SUTVA}). \end{aligned}$$

Similar to Section 2.2, we let  $m_a(X) = \mathbb{E}\{Y^{-1} \circ \lambda | A = a, X\}$ , so that  $\Delta^\lambda = \sum_{a=0,1} (2a - 1)\mathbb{E}_X m_a(X)$ . We consider a regression model  $m_a(X; \beta)$ , where  $\beta$  may be finite or infinite dimensional. In principle, the reference distribution  $\lambda$  may be chosen to be any continuous distribution, including known distributions such as the uniform distribution on  $\mathcal{I}$ . When the potential outcomes are continuous distributions, common choices of  $\lambda$  include the mean potential outcome  $\mu_a, a \in \{0, 1\}$ , the individual potential outcome  $Y_i(a), a \in \{0, 1\}$ , and the Wasserstein barycenter of the observed outcome  $\mu = \arg \min_{v \in \mathcal{W}_2(\mathcal{I})} \mathbb{E}\{W_2^2(Y, v)\}$ . In practice, the outcome  $Y_i$ , which is a distribution function itself, might not be fully observed. Instead, we typically only observe  $k_i$  samples from  $Y_i$ . We hence propose to construct the outcome regression estimator for  $\Delta^\lambda$  in four steps: (i) Use standard nonparametric methods such as the nonparametric maximum likelihood estimation, or local polynomial smoothing to obtain the estimates  $\widehat{Y}_i$ ; (ii) Obtain an estimate of  $\lambda$ , denoted as  $\hat{\lambda}$ ; for notational convenience, let  $\hat{\lambda} = \lambda$  if  $\lambda$  is a fixed or fully observed reference distribution; (iii) Regress  $\widehat{Y}^{-1} \circ \hat{\lambda}$  on  $X$  and  $A$  to obtain an estimate of  $m_a(X)$  for each individual in the sample, denoted as  $\hat{m}_a(X_i), i = 1, \dots, n$ ; (iv) Construct the outcome regression estimator via  $\hat{\Delta}_{OR}^{\hat{\lambda}} = \sum_{a=0,1} (2a - 1)\mathbb{P}_n \hat{m}_a(X)$ .

Following a similar discussion, we may construct an inverse probability weighting estimator

$$\hat{\Delta}_{IPW}^{\hat{\lambda}} = \sum_{a=0,1} (2a - 1)\mathbb{P}_n \frac{I(A = a)(\widehat{Y}^{-1} \circ \hat{\lambda})}{\hat{f}(A | X)}$$

and a doubly robust estimator

$$\hat{\Delta}_{DR}^{\hat{\lambda}} = \hat{\Delta}_{OR}^{\hat{\lambda}} + \sum_{a=0,1} (2a - 1)\mathbb{P}_n \left[ \frac{I(A = a)}{\hat{f}(A | X)} \{ \widehat{Y}^{-1} \circ \hat{\lambda} - \hat{m}_a(X) \} \right],$$

where  $\hat{f}(A | X)$  is an estimate of  $f(A | X)$ .

In practice, the doubly robust estimator is often preferable due to its double robustness. Moreover, it is possible to obtain root- $n$  consistency and asymptotic normality of  $\hat{\Delta}_{DR}^{\hat{\lambda}}$  under fairly general conditions on the nuisance estimates,  $\hat{\lambda}, \hat{m}_a(X)$  and  $\hat{f}(A | X)$ . In particular, these conditions allow for the use of flexible non-parametric methods for estimating the nuisance functions. We now formally establish these asymptotic results.

### 3.3 Asymptotic properties

To fix ideas, we consider  $\hat{\lambda} = \hat{\mu} := \arg \min_{v \in \mathcal{W}_2(\mathcal{I})} \frac{1}{n} \sum_{i=1}^n W_2^2(v, \widehat{Y}_i)$  in this part. Asymptotic analysis with other choices of  $\hat{\lambda}$  can be obtained in a similar fashion. In comparison to classical asymptotic

analyses of  $\hat{\Delta}_{DR}^\lambda$ , our analysis takes into account of the extra variability introduced by estimating  $Y_i, i = 1, \dots, n$  and  $\lambda$ . The following assumption characterizes this variability.

**Assumption 3.** *The estimates  $\hat{Y}_1, \dots, \hat{Y}_n$  are independent, and there are two sequences of constants  $\alpha_n = o(1)$  and  $\nu_n = o(1)$  such that*

$$\begin{aligned} \sup_{1 \leq i \leq n} \sup_{v \in \mathcal{W}_2(\mathcal{I})} \mathbb{E}\{W_2^2(\hat{Y}_i, Y_i) \mid Y_i = v\} &= O(\alpha_n^2), \\ \sup_{1 \leq i \leq n} \sup_{v \in \mathcal{W}_2(\mathcal{I})} \text{var}\{W_2^2(\hat{Y}_i, Y_i) \mid Y_i = v\} &= O(\nu_n^4). \end{aligned} \tag{11}$$

Assumption 3 requires that  $\hat{Y}_i, i = 1, \dots, n$  converge to their population counterparts at certain rates. Suppose that the number of observations for unit  $i$ ,  $k_i \asymp n^\zeta$  for some constant  $\zeta > 0$ . If  $\hat{Y}_i$  is obtained using the corresponding empirical distribution function, then under some additional moment assumptions, condition (S1) holds with  $\alpha_n^2 = \nu_n^4 = n^{-\zeta/2}$ . This can be shown via a combination of Fournier and Guillin (2015, Theorem 1) and Santambrogio (2015, Proposition 2.17). Assumption 3 also holds with many other standard non-parametric estimators for  $Y_i$ . For example, under some regularity conditions on the distribution of  $Y$ , the estimator by Petersen and Müller (2016) satisfies condition (S1) with a faster rate:  $\alpha_n^2 = n^{-2\zeta/3}$  and  $\nu_n^4 = n^{-4\zeta/3}$ .

The next assumption requires that the outcome regression estimates  $\hat{m}_a$  obtained using  $\hat{\mu}$  and  $\hat{Y}_i, i = 1, \dots, n$  are not too far way from the estimates  $\tilde{m}_a = m_a(X; \tilde{\beta})$  obtained by using the outcome  $Y_i, i = 1, \dots, n$  and  $\mu$ . As the values of  $\hat{m}_a$  reside in the space  $L^2(\mathcal{I}; \hat{\mu})$ , while the values of  $\tilde{m}_a$  reside in the space  $L^2(\mathcal{I}; \mu)$ , we apply the optimal transport between these two measures to  $\hat{m}_a$ , so that these two functions can be compared under the same norm. Assumption 4 holds for estimators  $\hat{m}_a(x)$  that are Lipschitz continuous functions of a weighted average of  $(\hat{Y}_1)^{-1} \circ \hat{\mu}, \dots, (\hat{Y}_n)^{-1} \circ \hat{\mu}$ . Examples include local polynomial estimators, and parametric estimators satisfying certain regularity conditions.

**Assumption 4.**  $\mathbb{P}_n \|\hat{m}_a(X) \circ (\hat{\mu}^{-1}) \circ \mu - \tilde{m}_a(X)\|_\mu^2 = O_P(W_2^2(\hat{\mu}, \mu) + \alpha_n^2 + \nu_n^2)$ .

Let  $\|\tilde{m}_a - m_a\|^2 = \int \|\tilde{m}_a(x) - m_a(x)\|_\mu^2 dF_X(x)$ , the integrated squared error of  $\tilde{m}_a$  for estimating  $m_a$ , where  $F_X$  denotes the probability measure induced by  $X$ . Similarly, the integrated squared error of  $\hat{\pi}$  for estimating  $\pi$  is denoted by  $\|\hat{\pi} - \pi\|_2^2 = \int |\hat{\pi}(x) - \pi(x)|^2 dF_X(x)$ . Let  $\varrho_\pi^2 := \mathbb{E}\|\hat{\pi} - \pi\|_2^2$  and  $\varrho_m^2 = \max\{\mathbb{E}\|\tilde{m}_0 - m_0\|^2, \mathbb{E}\|\tilde{m}_1 - m_1\|^2\}$ .

**Theorem 3.** *Suppose that the potential outcomes are continuous distribution functions. Suppose that Assumptions 1–4 hold, and that Assumption 6 in the appendix hold with  $\alpha_n = o(n^{-1/2})$  and  $\nu_n = o(n^{-1/2})$ , then*

(i)  $\|\hat{\Delta}_{DR}^{\hat{\mu}} \circ (\hat{\mu})^{-1} \circ \mu - \Delta^\mu\|_\mu = O_P(n^{-1/2} + n^{-1/2} \varrho_m^{1/2} + n^{-1/2} \varrho_\pi + \varrho_m \varrho_\pi);$

(ii) if  $\varrho_m \varrho_\pi = o(n^{-1/2})$ ,  $\varrho_m = o(1)$ ,  $\varrho_\pi = o(1)$ , then  $\sqrt{n} (\hat{\Delta}_{DR}^{\hat{\mu}} \circ (\hat{\mu})^{-1} \circ \mu - \Delta^\mu)$  converges to a centered Gaussian process with the same asymptotic distribution as

$$\sqrt{n}(\mathbb{P}_n - \mathbb{E}) \left[ \frac{A\{Y^{-1} \circ \mu - m_1(X)\}}{\pi(X)} + m_1(X) - \frac{(1-A)\{Y^{-1} \circ \mu - m_0(X)\}}{1-\pi(X)} - m_0(X) \right]. \quad (12)$$

The covariance function  $C(s, t)$  of the limit distribution of the random process (12) can be estimated by the sample covariance. Specifically, let  $V_i = \frac{A_i\{\hat{Y}_i^{-1} \circ \hat{\mu} - \hat{m}_1(X_i)\}}{\hat{\pi}(X_i)} + \hat{m}_1(X_i) - \frac{(1-A_i)\{\hat{Y}_i^{-1} \circ \hat{\mu} - \hat{m}_0(X_i)\}}{1-\hat{\pi}(X_i)} - \hat{m}_0(X_i)$ . Then the function  $\hat{C}(s, t) = n^{-1} \sum_{i=1}^n \{V_i(s) - \bar{V}(s)\} \{V_i(t) - \bar{V}(t)\}$  can be used to estimate  $C(s, t)$ , where  $s, t \in \mathcal{I}$  and  $\bar{V} = n^{-1} \sum_{i=1}^n V_i$ .

**Remark 1** (Double robustness). *Theorem 3 shows that the estimator  $\hat{\Delta}_{DR}^{\hat{\mu}}$  enjoys the double robustness property: the convergence rate is  $n^{-1/2}$  when either of  $\varrho_\pi$  and  $\varrho_m$  is of the order  $n^{-1/2}$  and the other one is bounded. Moreover, one may use flexible non-parametric methods for estimating  $m_a, a = 0, 1$  and  $\pi$ , provided that the nonparametric convergence rates satisfy  $\varrho_m \varrho_\pi = o(n^{-1/2})$ .*

## 4 Extension to Manifold-valued Outcomes

### 4.1 Causal effect definition

Similar to Wasserstein space  $\mathcal{W}_2(\mathcal{I})$ , in general a Riemannian manifold is not a linear space, so expectation and subtraction are not well-defined. Motivated by discussions in Section 3, we project the Riemannian manifold to a linear tangent space, and define the causal effect via the projection. The main challenge in this extension is that in general, the Riemannian logarithmic map that maps an element on a Riemannian manifold to a tangent space may not always be well-defined. For example, the Riemannian logarithmic map at the north pole of  $\mathbb{S}^2$  is not (uniquely) defined for the south pole, as there are infinitely many shortest paths connecting the north and south poles.

Several conditions are hence necessary to define the Riemannian logarithmic map. These conditions are different depending on how close the Riemannian manifold is to being flat, characterized by the curvature of the Riemannian manifold. Unless otherwise noted, here curvature is defined in the Alexandrov sense, the precise definition of which is given in the

Supplementary Material. To provide some intuition, we note that the curvature of the sphere, plane, and hyperboloid is positive, zero and negative, respectively. The following proposition gives conditions under which the Riemannian exponential map is invertible. It is an analogue of Proposition 1 in a connected Riemannian manifold, and is included as part of Lemma 4 in the Supplementary Material.

**Assumption 5.** *The Riemannian manifold  $\mathcal{M}$  satisfies one of the following two conditions:*

- (a)  *$\mathcal{M}$  is a Hadamard manifold, i.e., a complete and simply connected Riemannian manifold of everywhere nonpositive curvature;*
- (b)  *$\mathcal{M}$  is a simply connected closed subspace of a complete Riemannian manifold of everywhere positive curvature upper bounded by  $\kappa > 0$  and the diameter of  $\mathcal{M}$  is less than  $\pi/(2\sqrt{\kappa})$ , where the diameter is defined by  $\sup_{\lambda_1, \lambda_2 \in \mathcal{M}} d(\lambda_1, \lambda_2)$ .*

**Proposition 4.** *Suppose that the Riemannian  $\mathcal{M}$  satisfies Assumption 5. Then the Riemannian logarithmic map  $\mathcal{L}_\lambda$  is well-defined for  $\lambda \in \mathcal{M}$ . As a result, for any  $\lambda \in \mathcal{M}$ , there is a one-to-one correspondence between  $\mathcal{M}$  and  $\mathcal{L}_\lambda(\mathcal{M}) := \{\mathcal{L}_\lambda z : z \in \mathcal{M}\} \subset T_\lambda \mathcal{M}$ . In addition, for a set of points  $\lambda_1, \dots, \lambda_n \in \mathcal{M}$ , let  $d(\lambda_i, \lambda)$  denote the distance between  $\lambda_i$  and  $\lambda$  defined in the Supplementary Material. Then their Fréchet mean  $\bar{\lambda}$ , defined as the point  $\lambda$  that minimizes  $\frac{1}{n} \sum_{i=1}^n d^2(\lambda_i, \lambda)$ , exists and is always unique. Moreover,  $\bar{\lambda}$  is the unique point in  $\mathcal{M}$  that satisfies  $\frac{1}{n} \sum_{i=1}^n \mathcal{L}_{\bar{\lambda}}(\lambda_i) = 0$ .*

Given Proposition 4, a natural extension of the causal effect maps in Section 3, and in particular those as defined in Interpretation 4, is given as follows.

**Definition 2.** *Let  $\mathcal{M}$  be a Riemannian manifold satisfying Assumption 5, and  $\lambda$  be any element on  $\mathcal{M}$ . The individual causal effect vector of  $A$  on  $Y$  is defined as*

$$\Delta_i^\lambda = \mathcal{L}_\lambda Y_i(1) - \mathcal{L}_\lambda Y_i(0), \quad (13)$$

where  $\mathcal{L}_\lambda$  denotes the Riemannian logarithmic map at  $\lambda$ . The (average) causal effect vector of  $A$  on  $Y$  is defined as

$$\Delta^\lambda = \mathbb{E} \mathcal{L}_\lambda Y(1) - \mathbb{E} \mathcal{L}_\lambda Y(0). \quad (14)$$

All causal effect vectors reside in the tangent space  $T_\lambda \mathcal{M}$ .

**Example 2** (Diffusion tensors). *Diffusion tensor imaging, which characterizes the microstructure of brain white matter, is widely used in the study of the neurological disorders such as Alzheimer's*

disease (e.g. Stebbins and Murphy, 2009). It is thus of interest to quantify the effect of an exposure on diffusion tensors. The space of diffusion tensors  $\text{Sym}^+(3)$ , consisting of  $3 \times 3$  symmetric positive-definite matrices, is not linear. Instead, it can be viewed as a smooth manifold in which the tangent space at  $Q \in \text{Sym}^+(3)$  is the space  $\text{Sym}(3)$  of  $3 \times 3$  symmetric matrices. It is furthermore a Hadamard manifold satisfying Assumption 5(a) under various definitions of Riemannian metric (Arsigny et al., 2007; Moakher, 2005; Pennec, 2006; Lin, 2019). See the simulations in Section 5.2 for additional discussions.

**Example 3** (Compositional data). Scientists are often interested in studying the effect of a certain exposure, such as a drug on gut microbiome composition (e.g. Vich Vila et al., 2020). The microbiome composition is often represented by the percentage of the amount of each microorganism in the gut, and thus is a vector whose entries are non-negative and sum to one. Stephens (1982) proposed to transform the composition vector by taking square-root of each coordinate and treat the transformed vector as a point in the positive quadrant of the  $p$ -dimensional sphere  $\mathbb{S}^p$  when there are  $p+1$  species of microorganisms under consideration. The sphere  $\mathbb{S}^p$  is a Riemannian manifold whose curvature is one everywhere, and any geodesically convex closed subset of diameter less than  $\pi/2$  satisfy Assumption 5(b). The tangent space at  $\lambda$ , as illustrated in Figure S2 in the Supplementary Material, is a  $p$ -dimensional tangent plane in  $\mathbb{R}^{p+1}$  that passes through  $\lambda$ . The corresponding Riemannian exponential map is  $\mathcal{E}_\lambda(v) = \cos(\|v\|)\lambda + \sin(\|v\|)v/\|v\|$  for  $v \in T_\lambda\mathbb{S}^p$ , where  $\|v\|$  denotes the norm in  $\mathbb{R}^{p+1}$ .

## 4.2 Identification and Estimation

Identification of the average causal effect vector for manifold-valued outcomes may be achieved under a similar set of conditions to Theorem 2.

**Theorem 4.** Under Assumptions 1, 2 and 5, for  $a = 0, 1$ , the average causal effect vector  $\Delta^\lambda$  is identifiable and is given by

$$\Delta^\lambda = \sum_{a=0,1} (2a-1) \mathbb{E}_X \{ \mathbb{E}[\mathcal{L}_\lambda Y \mid A = a, X] \} = \sum_{a=0,1} (2a-1) \mathbb{E} \left\{ \frac{I(A=a)\mathcal{L}_\lambda Y}{P(A=a \mid X)} \right\}. \quad (15)$$

If as in Interpretation 4, we let  $\mathcal{L}_\lambda Y = Y^{-1} \circ \lambda$  for  $Y, \lambda \in \mathcal{W}_2(\mathcal{I})$ , then Theorem 4 coincides with Theorem 2. In this sense, (15) provides a unified identification formula for outcomes defined on a Wasserstein space, or Riemannian manifolds satisfying Assumption 5. Theorem 4 can be established via the same arguments made in Section 3.2. Furthermore, the average causal effect vector can be estimated using the three estimators introduced in Section 3.2, by replacing

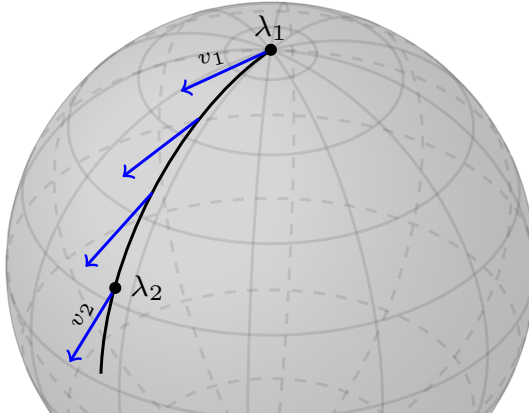


Figure 3: Illustration of parallel transport. The tangent vector  $v_1$  at  $\lambda_1$  is parallelly transported to the tangent vector  $v_2$  at  $\lambda_2$  along the geodesic connecting  $\lambda_1$  and  $\lambda_2$ .

$\widehat{Y}^{-1} \circ \hat{\lambda}$  with  $\mathcal{L}_{\hat{\lambda}} \widehat{Y}$ . We use the same notations  $\hat{\Delta}_{OR}^{\hat{\lambda}}$ ,  $\hat{\Delta}_{IPW}^{\hat{\lambda}}$  and  $\hat{\Delta}_{DR}^{\hat{\lambda}}$  to simplify the presentation of inference results.

Similar to Section 3.3, here we focus on studying asymptotic properties of the doubly robust estimator  $\hat{\Delta}_{DR}^{\hat{\lambda}}$ , and let  $\hat{\lambda} = \hat{\mu}$ . Here  $\hat{\mu}$  is the sample version of the Fréchet mean  $\mu$  of  $Y$ :  $\mu := \arg \min_{\lambda \in \mathcal{M}} \mathbb{E} d^2(\lambda, Y)$ , under the assumption that  $\mathbb{E} d^2(\lambda, Y) < \infty$  for some  $\lambda \in \mathcal{M}$ .

To quantify the estimation error, it may be tempting to use  $\hat{\Delta}_{DR}^{\hat{\mu}} - \Delta^\mu$ . However, this difference is not well defined: since  $\Delta^\mu \in T_\mu \mathcal{M}$  while  $\hat{\Delta}_{DR}^{\hat{\mu}} \in T_{\hat{\mu}} \mathcal{M}$ , they reside in different spaces. An intrinsic way to compare tangent vectors from different tangent spaces is to utilize the so-called parallel transport (Lin and Yao, 2019). A parallel transporter, determined by any two points  $\lambda_1, \lambda_2 \in \mathcal{M}$  and a path connecting them, moves vectors from the tangent space  $T_{\lambda_1} \mathcal{M}$  to  $T_{\lambda_2} \mathcal{M}$  in a smooth way; see Figure 3 for a graphical illustration, and the Supplementary Material for a more detailed description. A canonical choice for the path is the shortest path connecting the two points. Such parallel transporter, denoted by  $\tau_{\lambda_1}^{\lambda_2}$ , is uniquely determined by the points  $\lambda_1, \lambda_2$  and the Riemannian structure. Using this notation, we quantify the difference between  $\hat{\Delta}_{DR}^{\hat{\mu}}$  and  $\Delta^\mu$  by  $\tau_{\hat{\mu}}^\mu \hat{\Delta}_{DR}^{\hat{\mu}} - \Delta^\mu$ .

The following theorem extends Theorem 3 from  $\mathcal{W}_2(\mathcal{I})$  to Riemannian manifolds satisfying Assumption 5. In particular,  $\hat{\Delta}_{DR}^{\hat{\mu}} \circ \hat{\mu}^{-1} \circ \mu$  in Theorem 3 may be viewed as the parallel transport of  $\hat{\Delta}_{DR}^{\hat{\mu}}$  from the tangent space at  $\hat{\mu} \in \mathcal{W}_2(\mathcal{I})$  to the tangent space at  $\mu \in \mathcal{W}_2(\mathcal{I})$  along the shortest path connecting  $\hat{\mu}$  and  $\mu$  on  $\mathcal{W}_2(\mathcal{I})$ .

**Theorem 5.** *Under Assumptions 1–2, 5–6 and the additional Assumptions 7–9 in the Supplementary Material, we have*

$$(i) \quad \|\tau_{\hat{\mu}}^\mu \hat{\Delta}_{DR}^{\hat{\mu}} - \Delta^\mu\|_\mu = O_P(n^{-1/2} + n^{-1/2} \varrho_m^{1/2} + n^{-1/2} \varrho_\pi + \varrho_m \varrho_\pi);$$

(ii) if  $\varrho_m \varrho_\pi = o(n^{-1/2})$ ,  $\varrho_m = o(1)$ ,  $\varrho_\pi = o(1)$ , then  $\sqrt{n}(\tau_{\hat{\mu}}^\mu \hat{\Delta}_{DR}^{\hat{\mu}} - \Delta^\mu)$  converges to a centered Gaussian process that has the same asymptotic distribution as

$$\sqrt{n}(\mathbb{E}_n - \mathbb{E}) \left[ \frac{A\{\mathcal{L}_\mu Y - m_1(X)\}}{\pi(X)} + m_1(X) - \frac{(1-A)\{\mathcal{L}_\mu Y - m_0(X)\}}{1-\pi(X)} - m_0(X) + (\mathcal{Q}_1 - \mathcal{Q}_0)\mathcal{H}\mathcal{L}_\mu Y \right], \quad (16)$$

where  $\mathcal{H}$ ,  $\mathcal{Q}_1$  and  $\mathcal{Q}_0$  are linear operators (defined in the proof of the theorem) on  $T_\mu \mathcal{M}$ . It holds that  $\mathcal{Q}_1 = \mathcal{Q}_0$  when the curvature of  $\mathcal{M}$  is constantly zero.

**Remark 2.** When the curvature of  $\mathcal{M}$  is constantly zero, e.g., when  $\mathcal{M}$  is the manifold of symmetric positive-definite matrices endowed with either the Log-Euclidean metric (Arsigny et al., 2007) or the Log-Cholesky metric (Lin, 2019), (16) is simplified to

$$\sqrt{n}(\mathbb{E}_n - \mathbb{E}) \left[ \frac{A\{\mathcal{L}_\mu Y - m_1(X)\}}{\pi(X)} + m_1(X) - \frac{(1-A)\{\mathcal{L}_\mu Y - m_0(X)\}}{1-\pi(X)} - m_0(X) \right].$$

Similarly, the additional term  $(\mathcal{Q}_1 - \mathcal{Q}_0)\mathcal{H}\mathcal{L}_\mu Y$  in eqn. (16) does not show up in Theorem 3 because roughly speaking, the space  $\mathcal{W}_2(\mathcal{I})$  has zero curvature (Kloeckner, 2010).

## 5 Simulation studies

### 5.1 Wasserstein spaces

Our simulation data consist of  $n$  independent samples from the joint distribution of  $(X, A, Y)$ . The confounder  $X$  follows a uniform distribution on  $[-1, 1]$ . Conditional on  $X$ , the treatment  $A$  follows a Bernoulli distribution with mean  $P(A = 1 | X) = \text{expit}(1 + X)$ , where  $\text{expit}(\cdot) = \exp(\cdot)/(1 + \exp(\cdot))$ . The outcome  $Y$ , which is a random distribution function, is generated through the corresponding quantile function  $Y^{-1}(\alpha) = (-\mathbb{E}(A) + A + X + \epsilon) \sin(\pi\alpha)/8 + \alpha$ ,  $\alpha \in [0, 1]$ , where  $\epsilon$  is independently generated from a uniform distribution on  $[-0.5, 0.5]$ . Note that for any realization of  $X$  and  $A$ ,  $Y^{-1}(0) = 0$ ,  $Y^{-1}(1) = 1$ , and  $Y^{-1}(\alpha)$  is a continuous and strictly increasing function of  $\alpha$ , so that  $Y^{-1}$  is a quantile function for a continuous random variable taking values in  $\mathcal{I} = [0, 1]$ . It follows that  $Y \in \mathcal{W}_2(\mathcal{I})$ . Furthermore, since  $\mathbb{E}Y^{-1}(\alpha) = \alpha$ , the Wasserstein barycenter  $\mu$  is the uniform distribution on  $[0, 1]$ . We are interested in estimating  $\Delta^\mu(t) = \sin(\pi t)/8$ ,  $t \in \mathcal{I}$ .

The sample sizes are  $n = 50, 200, 1000$ . For each distribution function  $Y_i(t)$ ,  $t \in [0, 1]$ ,  $i = 1, \dots, n$ , we assume that we only have access to their values at  $t_j = 0.001 * (j - 1)$ ,  $j = 1, \dots, 1001$ . We estimated the outcomes  $Y_i$  with the empirical distribution functions  $\widehat{Y}_i$ , and the Wasserstein barycenter with  $\hat{\mu} = \left(\mathbb{P}_n \widehat{Y}_i^{-1}\right)^{-1}$ . We considered two specifications for the

outcome regression model: a linear regression model with predictor  $X$  in  $m_A(X)$  (correct) and a linear regression model with predictor  $X^2$  (incorrect), and two specifications for the propensity score model: a logistic regression model with predictor  $X$  (correct) and that with predictor  $X^2$  (incorrect). The estimation error is quantified using two measures: (1) bias of difference in medians:  $\Delta^{\hat{\mu}}(\hat{\mu}^{-1}(0.5)) - \Delta^{\mu}(\mu^{-1}(0.5))$ ; (2) root mean integrated squared error under the reference distribution  $\mu$ :  $\|\hat{\Delta}^{\hat{\mu}} \circ \hat{\mu}^{-1} \circ \mu - \Delta^{\mu}\|_{\mu}$ .

Table 1 summarizes the simulation results based on 1000 Monte Carlo replicates. The bias of difference in medians of the doubly robust estimator becomes closer to zero as the sample size increases when either the outcome regression or propensity score model is correct, thus confirming “double robustness.” In comparison, neither the OR or IPW estimator has the double robustness property: when the corresponding model is mis-specified, their bias of difference in medians can be large even at sample size 1000. Similar results hold for root mean integrated squared error. We further note that when the outcome resides in a Euclidean space, it is well-known that when both models are correct, the standard error of the OR estimator is no larger than that of the DR estimator, which is in turn no larger than that of the IPW estimator. One can see similar phenomenon from Table 1, where the outcome is a random distribution function residing in  $\mathcal{W}_2(\mathcal{I})$ .

## 5.2 Riemannian manifolds

In this part, we consider outcomes on the Riemannian manifold  $\mathcal{M} = \text{Sym}^+(3)$ , the space of  $3 \times 3$  symmetric positive-definite (SPD) matrices. When equipped with the Log-Cholesky metric (Lin, 2019),  $\mathcal{M}$  is a Hadamard manifold so that Assumption 5(a) holds. Specifically, our simulation data consist of  $n$  independent samples from the joint distribution of  $(X, A, Y)$ . The confounder  $X = (X_1, X_2)$  follows a bivariate normal distribution with mean 0 and  $\text{var}(X_1) = \text{var}(X_2) = 1$ ,  $\text{cov}(X_1, X_2) = 0.5$ . Conditional on  $X$ , the treatment  $A$  follows a Bernoulli distribution with mean  $P(A = 1 | X) = \text{expit}(0.5 + X_1 + X_2)$ . The outcome  $Y$ , which is a random  $3 \times 3$  SPD matrix, is generated from  $Y = \mathcal{E}_{\mu}\{(A - \mathbb{E}(A) + X_1)I_3 + X_21_3 + \varepsilon\}$ , where  $I_3$  is the  $3 \times 3$  identity matrix,  $1_3$  is the  $3 \times 3$  matrix with all entries equal to 1,  $\varepsilon$  is a random symmetric  $3 \times 3$  matrix whose lower triangular part follows the multivariate normal distribution  $N(0, I_6)$ ,  $\mu = I_3$  and  $\mathcal{E}_{\mu}$  denotes the Riemannian exponential map at  $\mu$  as detailed in the Supplementary Material. Note that for any realization of  $X$  and  $A$ ,  $\mathbb{E}\{(A - \mathbb{E}(A) + X_1)I_3 + X_21_3 + \varepsilon\} = 0$  so that following Proposition 4,  $\mathbb{E}Y = \mu$ .

The sample sizes are  $n = 50, 200, 1000$ . Here we assume the SPD matrices  $Y_i, i = 1, \dots, n$  are fully observed.  $\hat{\pi}(X)$  and  $\hat{m}_A(X)$  are obtained in a similar fashion as in Section 5.1. We implemented the OR, IPW and DR estimators. We considered two specifications for the

Table 1: Bias of difference in medians  $\times 100$  (standard error  $\times 100$ ) and root mean integrated squared error  $\times 100$  (standard error  $\times 100$ ) of three proposed estimators: the outcome regression estimator  $\hat{\Delta}_{OR}^{\hat{\mu}}$ , the inverse probability weighting estimator  $\hat{\Delta}_{IPW}^{\hat{\mu}}$ , and the doubly robust estimator  $\hat{\Delta}_{DR}^{\hat{\mu}}$ . The results are based on 1000 Monte Carlo replicates

Estimator	Model		Sample size		
	PS	OR	n=50	n=200	n=1000
Bias of difference in medians $\times 100$					
$\hat{\Delta}_{OR}^{\hat{\mu}}$	–	✓	-0.024(0.040)	0.023(0.018)	0.008(0.008)
$\hat{\Delta}_{OR}^{\hat{\mu}}$	–	✗	3.837(0.079)	3.952(0.038)	3.951(0.017)
$\hat{\Delta}_{IPW}^{\hat{\mu}}$	✓	–	0.016(0.045)	0.033(0.020)	0.005(0.009)
$\hat{\Delta}_{IPW}^{\hat{\mu}}$	✗	–	3.780(0.079)	3.884(0.037)	3.863(0.016)
$\hat{\Delta}_{DR}^{\hat{\mu}}$	✓	✓	-0.019(0.043)	0.019(0.019)	0.007(0.008)
$\hat{\Delta}_{DR}^{\hat{\mu}}$	✓	✗	0.152(0.065)	0.067(0.022)	0.007(0.010)
$\hat{\Delta}_{DR}^{\hat{\mu}}$	✗	✓	-0.028(0.041)	0.021(0.018)	0.008(0.008)
$\hat{\Delta}_{DR}^{\hat{\mu}}$	✗	✗	3.797(0.078)	3.885(0.037)	3.863(0.016)
Root mean integrated squared error $\times 100$					
$\hat{\Delta}_{OR}^{\hat{\mu}}$	–	✓	0.723(0.016)	0.323(0.008)	0.146(0.003)
$\hat{\Delta}_{OR}^{\hat{\mu}}$	–	✗	2.811(0.051)	2.793(0.027)	2.792(0.012)
$\hat{\Delta}_{IPW}^{\hat{\mu}}$	✓	–	0.789(0.020)	0.352(0.008)	0.159(0.004)
$\hat{\Delta}_{IPW}^{\hat{\mu}}$	✗	–	2.778(0.050)	2.746(0.026)	2.730(0.012)
$\hat{\Delta}_{DR}^{\hat{\mu}}$	✓	✓	0.763(0.018)	0.336(0.008)	0.151(0.004)
$\hat{\Delta}_{DR}^{\hat{\mu}}$	✓	✗	1.025(0.033)	0.395(0.010)	0.172(0.004)
$\hat{\Delta}_{DR}^{\hat{\mu}}$	✗	✓	0.735(0.017)	0.325(0.008)	0.146(0.003)
$\hat{\Delta}_{DR}^{\hat{\mu}}$	✗	✗	2.787(0.050)	2.746(0.026)	2.730(0.012)

outcome regression model: a linear regression model with predictors  $X_1$  and  $X_2$  in  $m_A(X)$  (correct) and a linear regression model with predictors  $X_1^2$  and  $X_2^2$  (incorrect), and two specifications for the propensity score model: a logistic regression model with predictor  $X_1$  and  $X_2$  (correct) and that with predictor  $X_1^2$  and  $X_2^2$  (incorrect). The estimation error is quantified using the following measures: (1) bias of mean diffusivity:  $MD(\hat{\Delta}^{\hat{\mu}}) - MD(\Delta^{\mu})$ , where the mean diffusivity of a  $3 \times 3$  symmetric matrix is the trace of the matrix divided by 3; (2) root mean squared error:  $\|\tau_{\hat{\mu}}^{\mu} \hat{\Delta}^{\hat{\mu}} - \Delta^{\mu}\|_{\mu}$ .

Table 2 summarizes the simulation results based on 1000 Monte Carlo simulation replicates. We see similar phenomena as in the case of Wasserstein spaces: the estimator  $\hat{\Delta}_{DR}^{\hat{\mu}}$  is doubly robust; when both the OR and PS models are correct, the OR estimator is more efficient than the DR estimator, which is more efficient than the IPW estimator.

## 6 Data Application

We apply our method to data obtained from the National Health and Nutrition Examination Survey (NHANES) 2005-2006<sup>1</sup>. The NHANES is a program of studies designed to assess the health and nutritional status of adults and children in the United States. The survey is unique in that it combines interviews and physical examinations. The NHANES interview includes demographic, socioeconomic, dietary, and health-related questions. The examination component consists of medical, dental, and physiological measurements, as well as laboratory tests administered by highly trained medical personnel.

In the 2005-2006 cycle of NHANES, participants of ages 6 years and older were asked to wear an Actigraph 7164 on a waist belt during all non-sleeping hours for seven days. The technology and application of current accelerometer-based devices in physical activity research allow the capture and storage or transmission of large volumes of raw acceleration signal data (Troiano et al., 2014). The NHANES accelerometer data have been widely used by researchers to explore relationships among accelerometer measures and a variety of other measures (Tudor-Locke et al., 2012). The monitors were programmed to begin recording activity information for successive 1 minute intervals (epochs) beginning at 12:01 a.m. the day after the health examination. The device was placed on an elasticized fabric belt, custom-fitted for each subject, and worn on the right hip. Subjects were told to keep the device dry (i.e. remove before swimming or bathing) and to remove the device at bedtime. For each participant, the physical activity intensity, ranging from 0 to 32767 cpm, was recorded every minute for 24 hours, 7 days.

The raw trajectory of activity intensity of the  $i$ th subject, denoted by  $Z_i(t)$ , was observed

---

<sup>1</sup><https://www.cdc.gov/nchs/nhanes/ContinuousNhances/Default.aspx?BeginYear=2005>.

Table 2: Bias of mean diffusivity (standard error) and root mean squared error (standard error) of three proposed estimators: the outcome regression estimator  $\hat{\Delta}_{OR}^{\hat{\mu}}$ , the inverse probability weighting estimator  $\hat{\Delta}_{IPW}^{\hat{\mu}}$ , and the doubly robust estimator  $\hat{\Delta}_{DR}^{\hat{\mu}}$ . The results are based on 1000 Monte Carlo replicates

Estimator	Model		Sample size		
	PS	OR	n=50	n=200	n=1000
Bias of mean diffusivity					
$\hat{\Delta}_{OR}^{\hat{\mu}}$	–	✓	0.136(0.038)	0.053(0.018)	0.007(0.008)
$\hat{\Delta}_{OR}^{\hat{\mu}}$	–	✗	6.019(0.123)	6.067(0.060)	5.964(0.027)
$\hat{\Delta}_{IPW}^{\hat{\mu}}$	✓	–	0.598(0.111)	0.152(0.056)	0.058(0.024)
$\hat{\Delta}_{IPW}^{\hat{\mu}}$	✗	–	6.190(0.126)	6.092(0.060)	5.913(0.026)
$\hat{\Delta}_{DR}^{\hat{\mu}}$	✓	✓	0.110(0.045)	0.063(0.020)	0.009(0.009)
$\hat{\Delta}_{DR}^{\hat{\mu}}$	✓	✗	0.981(0.122)	0.224(0.071)	0.093(0.031)
$\hat{\Delta}_{DR}^{\hat{\mu}}$	✗	✓	0.134(0.039)	0.054(0.017)	0.007(0.008)
$\hat{\Delta}_{DR}^{\hat{\mu}}$	✗	✗	6.145(0.125)	6.086(0.060)	5.913(0.026)
Root mean squared error					
$\hat{\Delta}_{OR}^{\hat{\mu}}$	–	✓	0.474(0.010)	0.121(0.003)	0.023(0.001)
$\hat{\Delta}_{OR}^{\hat{\mu}}$	–	✗	6.050(0.094)	5.943(0.046)	5.941(0.020)
$\hat{\Delta}_{IPW}^{\hat{\mu}}$	✓	–	2.418(0.617)	0.751(0.130)	0.140(0.017)
$\hat{\Delta}_{IPW}^{\hat{\mu}}$	✗	–	6.368(0.101)	5.989(0.045)	5.841(0.020)
$\hat{\Delta}_{DR}^{\hat{\mu}}$	✓	✓	0.863(0.076)	0.232(0.010)	0.043(0.002)
$\hat{\Delta}_{DR}^{\hat{\mu}}$	✓	✗	2.898(0.767)	0.974(0.141)	0.190(0.022)
$\hat{\Delta}_{DR}^{\hat{\mu}}$	✗	✓	0.496(0.011)	0.122(0.003)	0.023(0.001)
$\hat{\Delta}_{DR}^{\hat{\mu}}$	✗	✗	6.276(0.098)	5.979(0.045)	5.841(0.020)

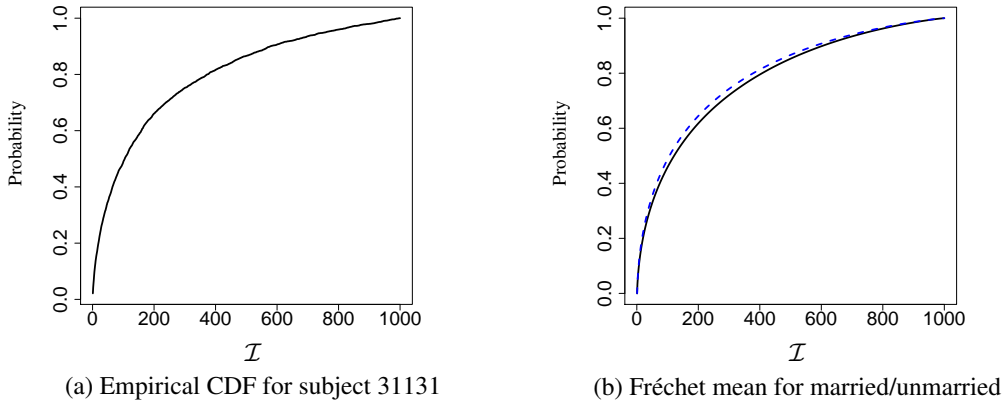


Figure 4: Panel (a) plots the preprocessed data for a randomly selected subject, where we transform the raw data to a cumulative distribution function in  $\mathcal{W}_2([1, 1000])$ . Panel (b) plots the Wasserstein barycenter of the empirical cumulative distribution functions for the married group (black solid line) and unmarried group (blue dashed line).

every minute, i.e.  $\{Z_{ij} = Z_i(t_j), \text{ with } t_j = j, 1 \leq j \leq 10080\}$ . Most intensity values are between 0 and 1000 cpm. Furthermore, the majority of intensity values are 0, corresponding to subjects sleeping or not wearing the device. To obtain robust and reliable results, we did the following preprocessing steps: (i) we excluded all observations that data reliability is questionable following NHANES protocol, after which there were 7170 subjects left; (ii) for each subject, we removed observations with intensity values higher than 1000 or equal to 0 (Chang and McKeague, 2020); (iii) we removed subjects with no more than 100 observations left, which further reduced the sample size to 7014. As different subjects have different circadian rhythms, we considered as outcome of interest the distribution of activity intensity that is invariant to circadian rhythms. As an example, in Figure 4(a), we plot the empirical cumulative distribution function for a random selected participant (subject ID 31131) who was 44 years old, female and married.

As discussed in Example 1, behavioral scientists are interested in knowing the causal effect of marriage on the physical activity. In our analysis, marriage was coded as a binary variable, with 1 being married or living with a partner, and 0 being otherwise. For illustrative purpose, we removed 1490 participants for whom we do not have information on their marriage status. This left us with 5524 participants in the analysis, with 2682 participants in the married group and 2842 participants in the unmarried group. Among these participants, the average age was 40.2 years old with standard deviation 21.3, and 52.3% of them were female. In Figure 4(b), we plot the Wasserstein barycenter of the empirical cumulative distribution functions for the married group and unmarried group, respectively. The Wasserstein barycenter in the married group is stochastically greater than that in the unmarried group, suggesting a positive association

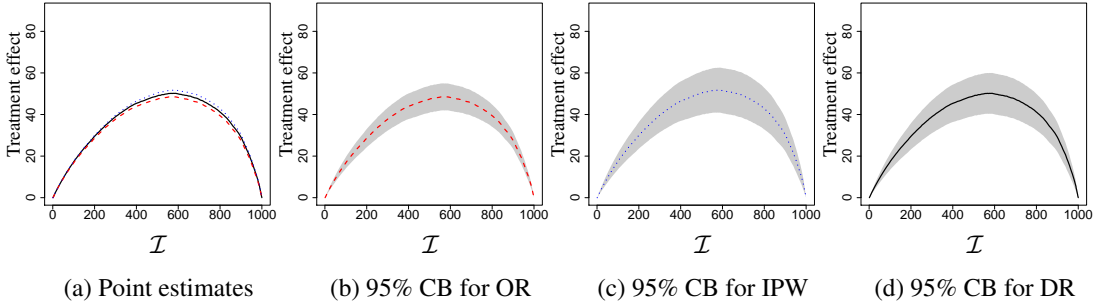


Figure 5: Causal effect estimates with the OR (red dashed), IPW (blue dotted) and DR (black solid) estimators: point estimates and 95% confidence bands. The reference distribution is chosen as the Wasserstein barycenter of observed outcomes.

between marriage and physical activity level. However, this crude association may be subject to potential confounders such as age and gender.

To adjust for these confounders, we applied the OR, IPW and DR estimators for estimating the average treatment effect  $\Delta^\lambda$ , where the reference distribution  $\lambda$  was chosen as the Wasserstein barycenter of the empirical CDFs for the participants. The corresponding estimates are plotted in Figure 5(a). To quantify the uncertainty of these estimates, we plot the corresponding 95% confidence bands in Figure 5 (b)–(d), where the confidence bands for IPW estimator and doubly robust estimator were obtained using the method proposed in Choi and Reimherr (2018), and the confidence band for the outcome regression estimator was obtained using the conventional linear regression confidence interval for the slope coefficient corresponding to the exposure  $A$ . One can see that the estimation results from the three methods are very close to each other, and the OR method has the tightest confidence band among the three methods.

Estimation results shown in Figure 5 suggest that after adjusting for age and gender, marriage has a significant positive causal effect on physical intensity level. According to the DR estimation results, for periods when their intensity level is at 400 cpm, marriage leads to an increase of 45.4 (95% CI = [37.8, 50.1]) cpm in their intensity level. Figure 6 shows the estimated difference in quantiles of the physical intensity distribution due to marriage:  $\hat{\Delta}^{\hat{\mu}} \circ \hat{\mu}^{-1}$ , corresponding to panel (c) in Figure 2. According to the DR estimation results, on average marriage leads to an increase of 19.1 (95% CI = [14.9, 23.3]) cpm in the median physical intensity level. In Figure 7(a) we plot the population causal transport map, estimated by  $\hat{\Delta}^{\hat{\mu}_0} + \text{id}$ . According to the DR estimation results, on average, an unmarried participant whose intensity level was at 400 cpm at a certain period, would have raised their intensity level to 444.9 cpm during the same period, had they got married. In Figure 7(b) we plot the individual causal transport map  $T_i$  for Subject 31131. Following Proposition 3,  $\Delta_i^{Y_i(1)} = \text{id} - T_i^{-1}$ . Since Subject 31131 was married,  $T_{31131}$  can

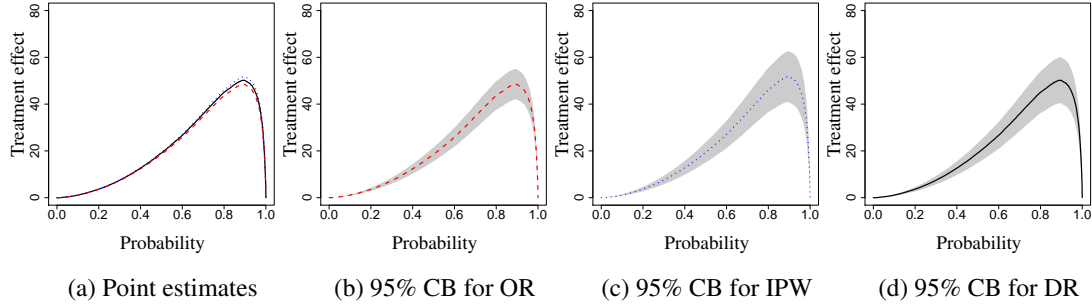


Figure 6: Difference in quantiles estimates with the OR (red dashed), IPW (blue dotted) and DR (black solid) estimators: point estimates and 95% confidence bands.

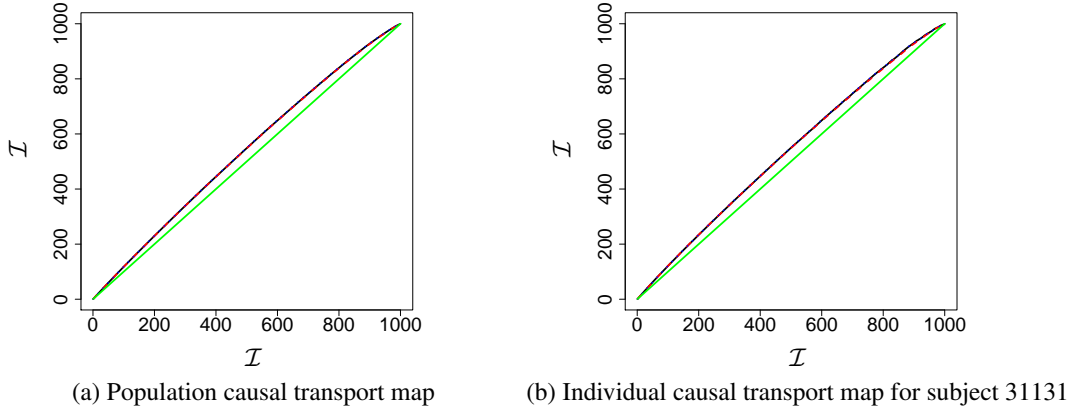


Figure 7: Estimates of the population causal transport map and the individual causal transport map for Subject 31131 with the OR (red dashed), IPW (blue dotted) and DR (black solid) estimators. For ease of comparison, we plot the 45 degree line in green, which corresponds to the null case of no treatment effect.

be estimated by  $\hat{T}_{31131} = (\text{id} - \hat{\Delta}^{\hat{Y}_{31131}})^{-1}$ . According to the DR estimation results, for periods that Subject 31131 had an intensity level of 500 cpm, her intensity level would have reduced to 451.6 cpm during the same period, had she not married.

## 7 Discussion

In this paper, we study causal inference for distribution functions and manifold-valued outcomes. We propose novel definitions of causal effects that satisfy several desiderata, and develop doubly robust estimation procedures for estimating these effects under the assumption of no unmeasured confounding. It would be interesting to extend classical causal inference methods

for dealing with unmeasured confounding, such as the instrumental variable methods (e.g. Ogburn et al., 2015; Wang and Tchetgen Tchetgen, 2018) to this setting. To the best of our knowledge, ours is the first formal study of causal effects for outcomes defined on a non-linear space. As such, we have only considered some leading special cases of non-linear spaces. There are many other data objects from non-linear spaces that we do not consider in this paper. For example, the Wasserstein spaces of probability distributions on higher dimensional Euclidean spaces exhibit structures different from  $\mathcal{W}_2(\mathcal{I})$  and thus poses new challenges for causal inference on such spaces. For data arising from a metric space in which the Riemannian logarithmic map does not exist, such as phylogenetic trees (Billera et al., 2001), causal inference is much more challenging and is an interesting topic for future exploration.

## Appendix: Regularity Conditions for Theorem 3

To study the asymptotic properties of the causal effect map estimator  $\hat{\Delta}_{DR}^{\hat{\mu}}$ , we introduce Assumption 6 that is standard in causal effect estimation, corresponding to the case where the outcomes  $Y_i, i = 1, \dots, n$  are fully observed. To state this assumption, we first introduce a Donsker class. Consider a fixed  $a \in \{0, 1\}$ . For a real number  $t \in \mathcal{I}$ , a function  $\check{m} : \mathcal{X} \rightarrow \mathcal{L}_\mu(\mathcal{W}_2(\mathcal{I})) := \{\mathcal{L}_\mu \lambda : \lambda \in \mathcal{W}_2(\mathcal{I})\}$  and a function  $\check{\pi} : \mathcal{I} \rightarrow \mathbb{R}$ , we view the element  $t \times \check{m} \times \check{\pi}$  as a real-valued function defined on  $(A, X, Y)$  by

$$(t \times \check{m} \times \check{\pi})(A, X, Y) = \frac{(aA + (1-a)(1-A))\{(Y^{-1} \circ \mu)(t) - \check{m}_a(X)(t)\}}{a\check{\pi}(X) + (1-a)(1-\check{\pi})} + \check{m}_a(X)(t),$$

and for a family  $\mathcal{F}_a$  of functions in the form of  $t \times \check{m} \times \check{\pi}$ , we view  $\sqrt{n}\mathcal{G}_a(t \times \check{m} \times \check{\pi}) := \sqrt{n}(\mathbb{P}_n - \mathbb{E})\{(t \times \check{m} \times \check{\pi})(A, X, Y)\}$  as a real-valued random process indexed by functions in  $\mathcal{F}_a$ . Let  $L^\infty(\mathcal{F}_a)$  denote the collection of real-valued functions  $H$  defined on  $\mathcal{F}_a$  and satisfying  $\sup_{q \in \mathcal{F}_a} |H(q)| < \infty$ . We say  $\mathcal{F}_a$  is a Donsker class if  $\sqrt{n}\mathbb{G}_a$  converges to a tight Gaussian measure on  $L^\infty(\mathcal{F}_a)$ .

Let  $\mathcal{M}_a$  be a class of functions and contains  $m_a$ . For  $g, h \in \mathcal{M}_a$ , define  $\eta_i(g, h) = \|g(X_i) - h(X_i)\|_\mu$  and  $\eta^2(g, h) = n^{-1} \sum_{i=1}^n \eta_i^2(g, h)$ . Conditional on  $\mathbb{X} = (X_1, \dots, X_n)$ ,  $\eta$  defines a pseudo-distance function on  $\mathcal{M}_a$ . Let  $B_a(r; g) = \{h \in \mathcal{M}_a : \eta(g, h) < r\}$  be a ball in  $\mathcal{M}_a$  with radius  $r$ , and  $N_a(\delta, r, \eta)$  denote the smallest number of  $\delta$ -balls in the pseudo-metric space  $(\mathcal{M}_a, \eta)$  that are required to cover  $B_a(r; m_a)$ . Without loss of generality, we assume  $N_a(\delta, r, \eta)$  is continuous in  $\delta$  and  $r$ . Otherwise, we just redefine it with its continuous upper bound.

### Assumption 6.

- (a) *The estimated propensity scores are bounded away from zero: for some  $\epsilon > 0$ ,  $\text{pr}\{\inf_x \hat{\pi}(x) > \epsilon \text{ and } \sup_x \hat{\pi}(x) < 1 - \epsilon\} = 1$ .*
- (b) *Stability of the estimators: For a constant  $C_4 > 0$ ,  $\sup_{1 \leq i \leq n} \mathbb{E}|\hat{\pi}(X_i) - \hat{\pi}_{-i}(X_i)|^2 \leq C_4 n^{-1}$  and  $\sup_a \sup_{1 \leq i \leq n} \mathbb{E}\|\tilde{m}_a(X_i) - \tilde{m}_{a,-i}(X_i)\|_\mu^2 \leq C_4 n^{-1}$ , where  $\hat{\pi}_{-i}$  and  $\tilde{m}_{a,-i}$  are the estimates of  $\pi$  and  $m_a$  without using the  $i$ th subject, respectively.*
- (c) *The outcome regression and propensity score estimates converge:  $\sup_x \|\tilde{m}_a(x) - m_a^*(x)\|_\mu = o_P(1)$ ,  $a = 0, 1$  and  $\sup_x |\hat{\pi}(x) - \pi^*(x)| = o_P(1)$  for some limit functions  $m_a^*$  and  $\pi^*$ .*
- (d) *For each  $a = 0, 1$ , the class  $\mathcal{F}_a$  is a Donsker class containing  $t \times m_a^* \times \pi^*$  for all  $t$ , and with probability tending to one  $t \times \tilde{m}_a \times \hat{\pi} \in \mathcal{F}_a$  for all  $t$ .*
- (e) *For  $a = 0, 1$ , for some fixed  $K > 0$ ,  $\tilde{m}_a \in \mathcal{M}_a$ ,  $\hat{m}(\cdot) \circ \hat{\mu}^{-1} \circ \mu \in \mathcal{M}_a$ , and  $\log N_a(\delta, r, \eta) \leq Kr\delta^{-1}$  for all  $r, \delta > 0$  almost surely.*

Part (e) in the above, controlling the complexity of the estimator  $\tilde{m}_a$ , is not needed if cross-fitting is used (e.g. Chernozhukov et al., 2018).

## SUPPLEMENTARY MATERIAL

The supplementary file contains additional background for Riemannian manifolds, additional regularity conditions for Theorem 5, additional details for simulation studies, technical lemmas and proofs for all the theorems.

## References

Aguech, M. and Carlier, G. (2011), “Barycenters in the Wasserstein space,” *SIAM Journal on Mathematical Analysis*, 43, 904–924.

Alimisis, F., Orvieto, A., Bécigneul, G., and Lucchi, A. (2020), “A Continuous-time Perspective for Modeling Acceleration in Riemannian Optimization,” in *Proceedings of the Twenty Third International Conference on Artificial Intelligence and Statistics, PMLR*, vol. 108, pp. 1297–1307.

Ambrosio, L., Gigli, N., and Savaré, G. (2004), “Gradient flows with metric and differentiable structures, and applications to the Wasserstein space,” *Atti della Accademia Nazionale dei Lincei. Classe di Scienze Fisiche, Matematiche e Naturali. Rendiconti Lincei. Serie IX. Matematica e Applicazioni*, 15, 327–343.

Ambrosio, L., Gigli, N., and Savare, G. (2005), *Gradient Flows*, Birkhäuser Basel.

Arsigny, V., Fillard, P., Pennec, X., and Ayache, N. (2007), “Geometric Means in a Novel Vector Space Structure on Symmetric Positive-Definite Matrices,” *SIAM Journal of Matrix Analysis and Applications*, 29, 328–347.

Bhattacharya, R. and Patrangenaru, V. (2003), “Large sample theory of intrinsic and extrinsic sample means on manifolds. I,” *The Annals of Statistics*, 31, 1–29.

— (2005), “Large sample theory of intrinsic and extrinsic sample means on manifolds. II,” *The Annals of Statistics*, 33, 1225–1259.

Bigot, J. (2020), “Statistical data analysis in the Wasserstein space,” *ESAIM: Proceedings and Surveys*, 68, 1–19.

Bigot, J., Gouet, R., Klein, T., and López, A. (2017), “Geodesic PCA in the Wasserstein space by convex PCA,” *Annales de l’Institut Henri Poincaré, Probabilités et Statistiques*, 53, 1–26.

Bigot, J., Imb, T. K., Imt, and Enac (2012), “Characterization of barycenters in the Wasserstein space by averaging optimal transport maps,” *Esaim: Probability and Statistics*, 22, 35–57.

Billera, L. J., Holmes, S. P., and Vogtmann, K. (2001), “Geometry of the Space of Phylogenetic Trees,” *Advances in Applied Mathematics*, 27, 733–767.

Bridson, M. R. and Häfliger, A. (1999), *Metric Spaces of Non-Positive Curvature*, Springer-Verlag.

Burago, D., Burago, Y., and Ivanov, S. (2001), *A Course in Metric Geometry*, Providence, RI: American Mathematical Society.

Chang, H.-W. and McKeague, I. W. (2020), “Nonparametric comparisons of activity profiles from wearable device data,” *preprint*.

Chernozhukov, V., Chetverikov, D., Demirer, M., Duflo, E., Hansen, C., Newey, W., and Robins, J. (2018), “Double/debiased machine learning for treatment and structural parameters,” *The Econometrics Journal*, 21, C1–C68.

Choi, H. and Reimherr, M. (2018), “A geometric approach to confidence regions and bands for functional parameters,” *Journal of the Royal Statistical Society: Series B (Statistical Methodology)*, 80, 239–260.

Cornea, E., Zhu, H., Kim, P., and Ibrahim, J. G. (2017), “Regression models on Riemannian symmetric spaces,” *Journal of the Royal Statistical Society: Series B (Statistical Methodology)*, 79, 463–482.

Cuturi, M. and Doucet, A. (2014), “Fast computation of Wasserstein barycenters,” *Proceedings of the 31st International Conference on Machine Learning (ICML)*, 32.

Eltzner, B. and Huckemann, S. F. (2019), “A smearly central limit theorem for manifolds with application to high-dimensional spheres,” *The Annals of Statistics*, 47, 3360–3381.

Fletcher, P. T. (2013), “Geodesic regression and the theory of least squares on Riemannian manifolds,” *International Journal of Computer Vision*, 105, 171–185.

Fournier, N. and Guillin, A. (2015), “On the rate of convergence in Wasserstein distance of the empirical measure,” *Probability Theory and Related Fields*, 162, 707–738.

Gray, A. (2004), *Tubes*, Springer Basel AG, 2nd ed.

Kendall, W. S. and Le, H. (2011), “Limit theorems for empirical Fréchet means of independent and non-identically distributed manifold-valued random variables,” *Brazilian Journal of Probability and Statistics*, 25, 323–352.

Kim, Y.-H. and Pass, B. (2017), “Wasserstein barycenters over Riemannian manifolds,” *Advances in Mathematics*, 307, 640–683.

King, A. C., Kiernan, M., Ahn, D. K., and Wilcox, S. (1998), “The effects of marital transitions on changes in physical activity: results from a 10-year community study,” *Annals of Behavioral Medicine*, 20, 64–69.

Kloeckner, B. (2010), “A geometric study of Wasserstein spaces: Euclidean spaces,” *Ann. Scuola Norm. Sup. Pisa Cl. Sci*, IX, 297–323.

Kuelbs, J. (1978), “Some Exponential Moments of Sums of Independent Random Variables,” *Transactions of the American Mathematical Society*, 240, 145–162.

Lee, J. (2018), *Introduction to Riemannian Manifolds*, Springer, 2nd ed.

Lee, J. M. (1997), *Riemannian Manifolds: An Introduction to Curvature*, New York: Springer-Verlag.

— (2009), *Manifolds and Differential Geometry*, Graduate Studies in Mathematics, American Mathematical Society.

Lin, Z. (2019), “Riemannian Geometry of Symmetric Positive Definite Matrices via Cholesky Decomposition,” *SIAM Journal on Matrix Analysis and Applications*, 40, 1353–1370.

Lin, Z. and Yao, F. (2019), “Intrinsic Riemannian functional data analysis,” *The Annals of Statistics*, 47, 3533–3577.

Mammen, E. and van de Geer, S. (1997), “Locally adaptive regression splines,” *Annals of Statistics*, 25, 387–413.

Moakher, M. (2005), “A differential geometry approach to the geometric mean of symmetric positive-definite matrices,” *SIAM Journal on Matrix Analysis and Applications*, 26, 735–747.

Ogburn, E. L., Rotnitzky, A., and Robins, J. M. (2015), “Doubly robust estimation of the local average treatment effect curve,” *Journal of the Royal Statistical Society: Series B (Statistical Methodology)*, 77, 373–396.

Patrangenaru, V. and Ellingson, L. (2015), *Nonparametric Statistics on Manifolds and Their Applications to Object Data Analysis*, CRC Press.

Pennec, X. (2006), “Intrinsic statistics on Riemannian manifolds: Basic tools for geometric measurements,” *Journal of Mathematical Imaging and Vision*, 25, 127–154.

— (2018), “Barycentric subspace analysis on manifolds,” 46, 2711–2746.

Petersen, A. and Müller, H.-G. (2016), “Functional data analysis for density functions by transformation to a Hilbert space,” *The Annals of Statistics*, 44, 183–218.

Petersen, A. and Müller, H.-G. (2019), “Fréchet Regression for Random Objects with Euclidean Predictors,” *The Annals of Statistics*, 47, 691–719.

Robins, J. M., Rotnitzky, A., and Zhao, L. P. (1994), “Estimation of regression coefficients when some regressors are not always observed,” *Journal of the American Statistical Association*, 89, 846–866.

Rubin, D. B. (1980), “Comment,” *Journal of the American Statistical Association*, 75, 591–593.

Santambrogio, F. (2015), *Optimal Transport for Applied Mathematicians*, Birkhäuser Basel.

Schötz, C. (2019), “Convergence rates for the generalized Fréchet mean via the quadruple inequality,” *Electronic Journal of Statistics*, 13, 4280–4345.

Stebbins, G. and Murphy, C. (2009), “Diffusion tensor imaging in Alzheimer’s disease and mild cognitive impairment,” *Behavioural Neurology*, 21, 39–49.

Stephens, M. A. (1982), “Use of the von Mises distribution to analyse continuous proportions,” *Biometrika*, 69, 197–203.

Sturm, K.-T. (2003), “Probability measures on metric spaces of nonpositive curvature,” in *Heat kernels and analysis on manifolds, graphs, and metric spaces (Paris, 2002)*, vol. 338 of *Contemporary Mathematics*, Providence, RI: American Mathematical Society, pp. 357–390.

Sun, Y., Flammarion, N., and Fazel, M. (2019), “Escaping from saddle points on Riemannian manifolds,” *arxiv*.

Troiano, R. P., McClain, J. J., Brychta, R. J., and Chen, K. Y. (2014), “Evolution of accelerometer methods for physical activity research,” *British Journal of Sports Medicine*, 48, 1019–1023.

Tudor-Locke, C., Camhi, S. M., and Troiano, R. P. (2012), “Peer reviewed: a catalog of rules, variables, and definitions applied to accelerometer data in the National Health and Nutrition Examination Survey, 2003–2006,” *Preventing Chronic Disease*, 9.

van de Geer, S. (1990), “Estimating a regression function,” *Annals of Statistics*, 18, 907–924.

Vermeulen, K. and Vansteelandt, S. (2015), “Bias-reduced doubly robust estimation,” *Journal of the American Statistical Association*, 110, 1024–1036.

Vich Vila, A., Collij, V., Sanna, S., Sinha, T., Imhann, F., Bourgonje, A. R., Mujagic, Z., Jonkers, D. M. A. E., Masclee, A. A. M., Fu, J., Kurilshikov, A., Wijmenga, C., Zhernakova, A., and Weersma, R. K. (2020), “Impact of commonly used drugs on the composition and metabolic function of the gut microbiota,” *Nature Communications*, 11, 362.

Villani, C. (2003), *Topics in optimal transportation*, no. 58, American Mathematical Soc.

Wang, L. and Tchetgen Tchetgen, E. (2018), “Bounded, efficient and multiply robust estimation of average treatment effects using instrumental variables,” *Journal of the Royal Statistical Society: Series B (Statistical Methodology)*, 80, 531–550.

Yuan, Y., Zhu, H., Lin, W., and Marron, J. S. (2012), “Local Polynomial Regression for Symmetric Positive Definite Matrices,” *Journal of Royal Statistical Society: Series B (Statistical Methodology)*, 74, 697–719.

Zhang, C., Kokoszka, P., and Petersen, A. (2020), “Wasserstein Autoregressive Models for Density Time Series,” *arXiv preprint arXiv:2006.12640*.

# Supplementary Material for “Causal Inference on Non-linear Spaces: Distribution Functions and Beyond

## Abstract

The supplementary file contains additional background for Riemannian manifolds, additional regularity conditions for Theorem 5, additional details for simulation studies, technical lemmas and proofs for all the theorems.

## 1 Additional Background on Riemannian Manifolds

Here we present the main concepts and results regarding Riemannian manifolds that are used in the main paper. We refer interested readers to Lee (1997, 2009) for textbook treatment of this subject.

**Definition 3** (Topological space). *A topological space is a set  $\mathcal{X}$  and a class of subsets of  $\mathcal{X}$ , called the open sets of  $\mathcal{X}$ , such that the class contains the empty set  $\emptyset$  and is closed under the formation of finite intersections and arbitrary unions.*

A function  $f : \mathcal{T}_1 \rightarrow \mathcal{T}_2$  between two topological spaces  $\mathcal{T}_1$  and  $\mathcal{T}_2$  is continuous if for every open set  $B \subset \mathcal{T}_2$ , the preimage  $f^{-1}(B)$  of  $B$  is open in  $\mathcal{T}_1$ . A homeomorphism is a continuous and one-to-one mapping whose inverse is also continuous. Two topological spaces are homeomorphic to each other if there exists a homeomorphism between them, and homeomorphic spaces share the same topological properties.

Although one can define a continuous function between topological spaces, the definition of derivatives relies on additional structure so that a topological space resembles a linear space, at least locally. Specifically, a manifold modeled on  $\mathbb{R}^q$  is a topological space so that at each point there is a neighborhood that is homeomorphic to  $\mathbb{R}^q$ , where  $q$  is called the dimension of the manifold.

**Definition 4** (Differentiable manifolds). *Let  $\mathcal{M}$  be a topological manifold modeled on  $\mathbb{R}^q$ . We say  $\mathcal{M}$  is a  $C^p$ -differentiable manifold ( $p \geq 1$ ), if there exists a collection  $\mathcal{A}$  of pairs  $(U_\alpha, \phi_\alpha)$  indexed by an index set  $J$  and satisfying the following axioms:*

- (a) *Each  $U_\alpha$  is an open subset of  $\mathcal{M}$  and  $\bigcup_{\alpha \in J} U_\alpha = \mathcal{M}$ , i.e., the domains together cover  $\mathcal{M}$ ;*
- (b) *Each  $\phi_\alpha$  is a bijection from  $U_\alpha$  onto an open subset  $\phi_\alpha(U_\alpha) = \{\phi_\alpha(x) \in \mathbb{R}^q : x \in U_\alpha\}$  of  $\mathbb{R}^q$ ;*

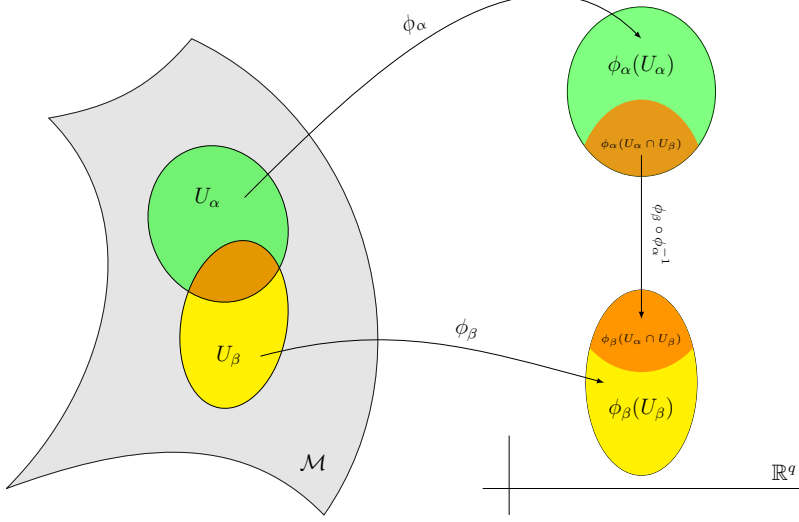


Figure S1: Illustration of the chart and transition map.

(c) For each pair  $\alpha, \beta \in J$ , if  $U_\alpha \cap U_\beta \neq \emptyset$ , then the  $p$ th derivative of the transition map  $\phi_\alpha \circ \phi_\beta^{-1} : \phi_\beta(U_\alpha \cap U_\beta) \rightarrow \phi_\alpha(U_\alpha \cap U_\beta)$  exists and is continuous; note that a transition map, as illustrated in Figure S1, is a mapping from a subset of  $\mathbb{R}^q$  to  $\mathbb{R}^q$ , so the derivatives of the transition map is defined in the ordinary sense. In this case, we say  $\phi_\alpha$  and  $\phi_\beta$  are compatible.

The pair  $(U_\alpha, \phi_\alpha)$  or sometimes  $\phi_\alpha$  itself is called a chart (or coordinate chart or coordinate map). The collection  $\mathcal{A}$  is called an atlas, which literally means a collection of charts. When  $p = 1$ , the manifold is called a differentiable manifold. When  $p = \infty$ , it is called a smooth manifold. Two atlases are equivalent or compatible if their union is again an atlas (satisfying the above three atlas axioms). An atlas is maximal if any other atlas compatible with it is contained in it. Each maximal atlas determines a differential structure on a given topological space, and conversely, each distinct differential structure is characterized by a unique maximal atlas.

Consider again the unit sphere  $\mathbb{S}^2 = \{(x_1, x_2, x_3) \in \mathbb{R}^3 : x_1^2 + x_2^2 + x_3^2 = 1\}$ . Let  $\mathcal{A} = \{(U_1, \phi_1), (U_2, \phi_2)\}$ , where  $U_1 = \mathbb{S}^2 \setminus \{(1, 0, 0)\}$  and  $U_2 = \mathbb{S}^2 \setminus \{(-1, 0, 0)\}$ , and

$$\begin{aligned}\phi_1(x_1, x_2, x_3) &= \frac{1}{1-x_1}(x_2, x_3) \in \mathbb{R}^2, \\ \phi_2(x_1, x_2, x_3) &= \frac{1}{1+x_1}(x_2, x_3) \in \mathbb{R}^2.\end{aligned}$$

One can check that  $\mathcal{A}$  is an atlas with which  $\mathbb{S}^2$  is a smooth manifold.

Let  $\mathcal{A}$  be a maximal atlas for a differentiable  $q$ -dimensional manifold  $\mathcal{M}$ . For  $\lambda \in \mathcal{M}$ , assume that  $(U, \phi) \in \mathcal{A}$  is chart such that  $\lambda \in U$ . Now for a curve  $\gamma : I \rightarrow U$  with  $\gamma(t) = \lambda$  for some  $t \in I$ , we say  $\gamma$  is differentiable at  $t \in I$  if the composite function  $\phi \circ \gamma$  (which is a function mapping  $I$  into  $\mathbb{R}^q$ ) is differentiable at  $t$ . The curve  $\gamma$  is called a differentiable curve if it is differentiable at every  $t \in I$ . One can verify that this definition is independent of the chart, i.e., if  $\gamma$  is differentiable at  $t$  in a chart, then it is also differentiable at  $t$  in other charts that contain  $\gamma(t)$ . If  $\eta : J \rightarrow \mathcal{M}$  with  $\eta(s) = \lambda$  is another differentiable curve parameterized by an interval  $J$ , we say  $\gamma$  is equivalent to  $\eta$  at  $\lambda$  if the first derivatives of  $\phi \circ \gamma$  at  $t$  and  $\phi \circ \eta$  at  $s$  coincide. This defines an equivalence relation among differentiable curves on  $\mathcal{M}$  at  $\lambda$ , and such equivalence relation does not depend on the chart  $(U, \phi)$ , i.e., compatible charts give rise to the same equivalence classes.

**Definition 5** (Tangent space). *For each point  $\lambda \in \mathcal{M}$ , an equivalence class of curves at  $\lambda$  is called a tangent vector at  $\lambda$ , and the collection of the tangent vectors at  $\lambda$  is called the tangent space at  $\lambda$ , conveniently denoted by  $T_\lambda \mathcal{M}$ .*

We emphasize that equivalence classes are only defined with reference to a point  $\lambda$  on the manifold. Equivalence classes from different points, and hence tangent spaces at different points, are distinct. In particular, a differentiable curve  $\gamma$  might be in different equivalence classes in different points. However, at any given point  $\lambda \in \mathcal{M}$ , a curve  $\gamma$  only belongs to one equivalence class at  $\lambda$ . For instance, if  $\gamma(s) \neq \gamma(t)$  for  $s, t$ , then  $\gamma$  belongs to an equivalence class  $u$  at  $\gamma(s)$ , and belongs to an equivalence  $v$  at  $\gamma(t)$ . For a differentiable curve  $\gamma : I \rightarrow \mathcal{M}$ , for each  $t \in I$ , the tangent vector (equivalence class) at  $\lambda = \gamma(t)$  is denoted by  $\gamma'(t)$ .

Each tangent space is viewed as a  $q$ -dimensional linear space with the following canonical scalar multiplication and vector addition operations:

- **Scalar multiplication:** For a tangent vector  $v$  at  $\lambda$ , let  $\gamma : I \rightarrow \mathcal{M}$  be a curve from the equivalence class of  $v$  with  $\gamma(t) = \lambda$  for  $t \in I$ . For  $a \in \mathbb{R}$ , we define the scalar multiplication  $a \cdot v$  (abbreviated by  $av$ ) to be the equivalence class (tangent vector)  $u$  at  $\lambda$  such that, for any representative curve  $\eta : J \rightarrow \mathcal{M}$  in the equivalence class  $u$  with  $\eta(s) = \lambda$  for  $s \in J$ , for any chart  $(U, \phi)$  with  $\lambda \in U$ , the derivative  $(\phi \circ \eta)'$  of  $\phi \circ \eta$  at  $s$  is equal to  $a(\phi \circ \gamma)'(t)$ .
- **Vector addition:** For two tangent vectors  $v_1$  and  $v_2$  at  $\lambda$ , let  $\gamma_1 : I_1 \rightarrow \mathcal{M}$  and  $\gamma_2 : I_2 \rightarrow \mathcal{M}$  be two curves from their corresponding equivalence classes, respectively. Assume  $\gamma_j(t_j) = \lambda$  and  $t_j \in I_j$  for  $j = 1, 2$ . The vector addition  $v_1 + v_2$  of  $v_1$  and  $v_2$  is defined

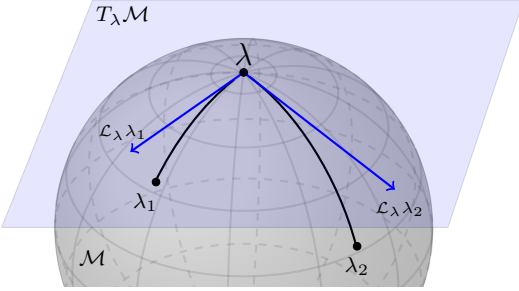


Figure S2: Illustration of geometric concepts of the Riemannian manifold. The segments from  $\lambda$  to  $\lambda_1$  and  $\lambda_2$  are geodesics connecting  $\lambda$  and  $\lambda_1$  and  $\lambda_2$ , respectively.

to be the equivalence class (tangent vector)  $u$  at  $\lambda$  such that, for any representative curve  $\eta : J \rightarrow \mathcal{M}$  in the equivalence class with  $\eta(s) = \lambda$  for  $s \in J$ , for any chart  $(U, \phi)$  with  $\lambda \in U$ , the derivative  $(\phi \circ \eta)'$  of  $\phi \circ \eta$  at  $s$  is equal to  $(\phi \circ \gamma_1)'(t_1) + (\phi \circ \gamma_2)'(t_2)$ .

Although tangent vectors are rigorously defined as equivalence classes, one often perceives them as vectors in a  $q$ -dimensional linear space, and in particular, identifies them with  $\mathbb{R}^q$ , or even visualizes the whole tangent space in a Euclidean space with a dimension larger than  $q$  for some manifolds. For example, the tangent space at point  $\mu \in \mathbb{S}^2$  can be visualized as the tangent plane at that point, that is  $T_\mu \mathbb{S}^2 = \{v \in \mathbb{R}^3 : v \cdot \lambda = 0\}$ , where  $\cdot$  denotes the dot product on  $\mathbb{R}^3$ ; see Figure S2 for an illustration.

**Definition 6** (Riemannian manifold). *A Riemannian manifold  $\mathcal{M}$  is a real, smooth manifold equipped with an inner product  $g_\lambda$  on the tangent space  $T_\lambda \mathcal{M}$  at each point  $\lambda$  that varies smoothly from point to point. If  $\mathcal{M}$  is also connected in the sense that it cannot be represented as the union of two or more disjoint non-empty open subsets, then we say  $\mathcal{M}$  is a connected Riemannian manifold.*

A connected Riemannian manifold  $\mathcal{M}$  is a metric space with the distance function induced collectively by the inner products  $g_\lambda$ . If  $\gamma : [a, b] \rightarrow \mathcal{M}$  is a continuously differentiable curve in the Riemannian manifold  $\mathcal{M}$ , then we define its length  $L(\gamma)$  by

$$L(\gamma) = \int_a^b \|\gamma'(t)\|_{\gamma(t)} dt,$$

where the notation  $\|\cdot\|_\lambda$  denotes the norm induced by the inner product  $g_\lambda$  on the tangent space  $T_\lambda \mathcal{M}$  for a generic  $\lambda \in \mathcal{M}$ . A *geodesic* on  $\mathcal{M}$  is a function  $\gamma : \mathbb{R} \rightarrow \mathcal{M}$  such that for all  $t \in \mathbb{R}$ , for sufficiently small  $\epsilon > 0$ , the segment  $\gamma([t, t + \epsilon])$  is the shortest path connecting  $\gamma(t)$  and  $\gamma(t + \epsilon)$ , and the length of the segment  $\gamma([t, t + \epsilon])$  is proportional to  $\epsilon$ . The distance  $d$  of two points is the length of the shortest geodesic in  $\mathcal{M}$  that connects the two points.

If the connected Riemannian manifold  $\mathcal{M}$  is complete, then by the Hopf-Rinow theorem, we can define a mapping from any vector in the tangent space  $T_\lambda \mathcal{M}$  to a point in  $\mathcal{M}$ , known as the Riemannian exponential map. For any vector  $v \in T_\lambda \mathcal{M}$ , there is a unique geodesic  $\gamma$  such that  $\gamma(0) = \lambda$  and  $\gamma'(0) = v$ . Then the Riemannian exponential map of  $v$  is defined by  $\mathcal{E}_\lambda v = \gamma(1)$ . Intuitively, if one starts from  $\lambda$  on  $\mathcal{M}$  in the direction of  $v$ , and then moves “forward” for a unit time, then it reaches  $\mathcal{E}_\lambda v$ . In general, the Riemannian exponential map may not be invertible, as there may be multiple geodesics between two points on  $\mathcal{M}$ . When  $\mathcal{E}_\lambda$  is invertible, its inverse, denoted as the Riemannian logarithmic map  $\mathcal{L}_\lambda \tilde{\lambda}$ , maps an element  $\tilde{\lambda}$  in  $\mathcal{M}$  to a vector in  $T_\lambda \mathcal{M}$ . Specifically, if there is a unique geodesic  $\gamma$  connecting  $\lambda$  and  $\tilde{\lambda}$  with  $\gamma(0) = \lambda$  and  $\gamma(1) = \tilde{\lambda}$ , then the Riemannian logarithmic map  $\mathcal{L}_\lambda \tilde{\lambda} := \gamma'(0)$ ; see Figure S2 for an illustration.

Unlike the linear space, a Riemannian manifold, or more generally, a metric space, is usually not flat, and the concept of curvature is used to measure the amount of deviation from being flat. An intuitive approach to introducing curvature is to compare geodesic triangles on the metric space to those on the following reference/model spaces  $M_\kappa^2$ :

- When  $\kappa = 0$ ,  $M_\kappa^2 = \mathbb{R}^2$  with the standard Euclidean distance  $\bar{d}_\kappa$ ;
- When  $\kappa < 0$ ,  $M_\kappa^2$  is the hyperbolic space  $\mathbb{H}^2 = \{(x, y, z) \in \mathbb{R}^3 : x^2 + y^2 - z^2 = -1 \text{ and } z > 0\}$  with the hyperbolic distance function  $\bar{d}_\kappa(p, q) = \cosh^{-1}(z_p z_q - x_p x_q - y_p y_q)/\sqrt{-\kappa}$ , where  $p = (x_p, y_p, z_p)$  and  $q = (x_q, y_q, z_q)$ ;
- When  $\kappa > 0$ ,  $M_\kappa^2$  is the sphere  $\mathbb{S}^2 = \{(x, y, z) \in \mathbb{R}^3 : x^2 + y^2 + z^2 = 1\}$  with the angular distance function  $\bar{d}_\kappa(p, q) = \cos^{-1}(x_p x_q + y_p y_q + z_p z_q)/\sqrt{\kappa}$ .

A geodesic triangle with vertices  $p, q, r$  in a metric space  $\mathcal{M}$ , denoted by  $\triangle(p, q, r)$ , consists of three minimizing geodesic segments that connect  $p$  to  $q$ ,  $p$  to  $r$  and  $q$  to  $r$ , respectively. A comparison triangle of  $\triangle(p, q, r)$  in the reference space  $M_\kappa^2$  is a geodesic triangle on  $M_\kappa^2$  formed by vertices  $\bar{p}, \bar{q}, \bar{r}$  such that  $d(p, q) = \bar{d}_\kappa(\bar{p}, \bar{q})$ ,  $d(p, r) = \bar{d}_\kappa(\bar{p}, \bar{r})$ , and  $d(q, r) = \bar{d}_\kappa(\bar{q}, \bar{r})$ , where  $\bar{d}_\kappa$  denotes the distance function on  $M_\kappa^2$ . In addition, if we use  $\bar{pq}$  to denote the minimizing geodesic connecting two points  $p, q$  on a manifold, then every point  $x$  on the geodesic  $\bar{pq}$  ( $\bar{pr}$ , respectively) has a counterpart  $\bar{x}$  on the geodesic segment  $\bar{pq}$  ( $\bar{pr}$ , respectively) of the comparison triangle such that  $d(p, x) = \bar{d}_\kappa(\bar{p}, \bar{x})$ . We say the *curvature in the Alexandrov sense* is lower (upper, respectively) bounded by  $\kappa$  at  $\lambda \in \mathcal{M}$  if and only if there exists an open set  $U_\lambda$  such that for every geodesic triangle  $\triangle(p, q, r)$  that is contained in  $U_\lambda$ , its comparison triangle  $\triangle(\bar{p}, \bar{q}, \bar{r})$  in  $M_\kappa^2$  satisfies the following property: if  $x \in \bar{pq}$ ,  $y \in \bar{pr}$ , then  $d(x, y) \geq \bar{d}_\kappa(\bar{x}, \bar{y})$  ( $d(x, y) \leq \bar{d}_\kappa(\bar{x}, \bar{y})$ , respectively). The space  $\mathcal{M}$  has lower (upper, respectively) bounded curvature  $\kappa$  if and only if the curvature is lower (upper, respectively) bounded by  $\kappa$  at every  $\lambda \in \mathcal{M}$ .

When analyzing data residing on a Riemannian manifold, one often needs to compare tangent vectors at different points. As mentioned previously, they can not be compared directly. One way to circumvent this difficulty is to utilize the concept of parallel transport that moves a tangent vector at a point into the tangent space at another point. The parallel transport is intrinsically dependent on the Riemannian structure of the manifold, and in particular, involves the so-called Levi–Civita covariant derivative, the precise definition of which can be found in Chapter 4 of Lee (1997). In general a parallel transport involves three ingredients: the starting point, the ending point, and a smooth path connecting the two points. A natural choice for the path is the unique minimizing geodesic between the points for the manifolds satisfying Assumption 5. When a vector is parallelly transported along the geodesic, its angle between the geodesic, as well as its length, remains constant, as illustrated in Figure 3. Intuitively, parallel transport does not induce distortion to the vector being transported, and this provides a meaningful comparison between tangent vectors from distinct tangent spaces.

## 2 Additional Assumptions for Theorem 5

The following assumption is in analogy to Assumption 3 when data are not fully observed.

**Assumption 7.** *The estimates  $\widehat{Y}_1, \dots, \widehat{Y}_n$  are independent, and there are two sequences of constants  $\alpha_n = o(n^{-1/2})$  and  $\nu_n = o(n^{-1/2})$  such that*

$$\begin{aligned} \sup_{1 \leq i \leq n} \sup_{v \in \mathcal{M}} \mathbb{E}\{d^2(\widehat{Y}_i, Y_i) \mid Y_i = v\} &= O(\alpha_n^2), \\ \sup_{1 \leq i \leq n} \sup_{v \in \mathcal{M}} \text{var}\{d^2(\widehat{Y}_i, Y_i) \mid Y_i = v\} &= O(\nu_n^4). \end{aligned} \tag{S1}$$

The following assumption imposes certain moment conditions on  $Y$  and  $\widehat{Y}$  when  $\mathcal{M}$  is a Hadamard space; such conditions are not required for manifolds  $\mathcal{M}$  characterized by Assumption 5(b) due to the finiteness of their diameters. Note that the condition  $\mathbb{E}d^2(p, Y) < \infty$  for some  $p \in \mathcal{M}$  ensures existence and uniqueness of the population Fréchet mean for a random element in a Hadamard space.

**Assumption 8.** *For  $\mathcal{M}$  characterized by Assumption 5(a), for some  $p \in \mathcal{M}$ ,  $\mathbb{E}d^2(p, Y) < \infty$ , and for some constant  $C_2 > 0$ ,  $\sup_{1 \leq i \leq n} \{\mathbb{E}d^8(Y_i, p) + \mathbb{E}d^8(\widehat{Y}_i, p)\} < C_2$ .*

**Assumption 9.**  $\mathbb{P}_n \|\tau_{\hat{\mu}}^\mu \hat{m}_a(X) - \tilde{m}_a(X)\|_\mu^2 = O_P(d^2(\hat{\mu}, \mu) + \alpha_n^2 + \nu_n^2).$

Finally, we reinterpret Assumption 6 in the following way. First,  $\|\cdot\|_\mu$  is interpreted as the norm in the tangent space  $T_\mu \mathcal{M}$ . To reinterpret the condition (d), we suppose that the manifold

$\mathcal{M}$  is of  $q$  dimensions. For a fixed  $a$ , for each positive integer  $k \leq q$ , a function  $\check{m} : \mathcal{X} \rightarrow T_\mu \mathcal{M}$  and a function  $\check{\pi} : \mathcal{I} \rightarrow \mathbb{R}$ , we view the element  $k \times \check{m} \times \check{\pi}$  as a real-valued function defined on  $(A, X, Y)$  by

$$(k \times \check{m} \times \check{\pi})(A, X, Y) = \frac{(aA + (1-a)(1-A))\{(Y^{-1} \circ \mu)(k) - \check{m}_a(X)(k)\}}{a\check{\pi}(X) + (1-a)(1-\check{\pi})} + \check{m}_a(X)(k),$$

where  $T_\mu \mathcal{M}$  is isometric to  $\mathbb{R}^q$  and  $\check{m}_a(X)(k)$  denotes the  $k$ th coordinate of  $\check{m}_a(X)$ . Now the family  $\mathcal{F}_a$  in the condition (d) contains functions in the form of  $k \times \check{m} \times \check{\pi}$ , and the corresponding random process is defined by  $\sqrt{n}\mathcal{G}_a(k \times \check{m} \times \check{\pi}) := \sqrt{n}(\mathbb{P}_n - \mathbb{E})\{(k \times \check{m} \times \check{\pi})(A, X, Y)\}$  for  $k \times \check{m} \times \check{\pi} \in \mathcal{F}_a$ . We say  $\mathcal{F}_a$  is a Donsker class if  $\mathbb{G}_a$  converges to a tight Gaussian measure on  $L^\infty(\mathcal{F}_a)$ .

### 3 Proof of Theorems 3 and 5

To simplify notation and unify the proofs, for  $\lambda, \nu \in \mathcal{W}_2(\mathcal{I})$ , write  $\mathcal{L}_\lambda \nu = \nu^{-1} \circ \lambda$  and

$$\tau_\lambda^\nu g = g \circ \lambda^{-1} \circ \nu \quad \text{for } g \in L^2(\lambda). \quad (\text{S2})$$

Also, let  $Z_i = \mathcal{L}_\mu Y_i$ ,  $\hat{Z}_i = \mathcal{L}_{\hat{\mu}} \hat{Y}_i$ ,  $R_i = \tau_{\hat{\mu}}^\mu \hat{Z}_i - Z_i$ , and  $D_a(x) = \tau_{\hat{\mu}}^\mu \hat{m}_a(x) - \check{m}_a(x)$ . The quantity  $R_i$  can be viewed as the residual due to the discrepancy between  $\hat{\mu}$  and  $\mu$ , and between  $\hat{Y}_i$  and  $Y_i$ . Define

$$\begin{aligned} \psi_1 &:= \mathbb{E} \left[ \frac{A\mathcal{L}_\mu Y}{\pi(X)} - \left\{ \frac{A}{\pi(X)} - 1 \right\} m_1(X) \right], \\ \psi_0 &:= \mathbb{E} \left[ \frac{(1-A)\mathcal{L}_\mu Y}{1-\pi(X)} - \left\{ \frac{1-A}{1-\pi(X)} - 1 \right\} m_0(X) \right] \end{aligned}$$

and their sample versions

$$\begin{aligned} \hat{\psi}_1 &:= \mathbb{P}_n \left[ \frac{A\mathcal{L}_{\hat{\mu}} \hat{Y}}{\hat{\pi}(X)} - \left\{ \frac{A}{\hat{\pi}(X)} - 1 \right\} \hat{m}_1(X) \right], \\ \hat{\psi}_0 &:= \mathbb{P}_n \left[ \frac{(1-A)\mathcal{L}_{\hat{\mu}} \hat{Y}}{1-\hat{\pi}(X)} - \left\{ \frac{1-A}{1-\hat{\pi}(X)} - 1 \right\} \hat{m}_0(X) \right]. \end{aligned}$$

Then we have  $\Delta^\mu = \psi_1 - \psi_0$  and  $\hat{\Delta}_{DR}^{\hat{\mu}} = \hat{\psi}_1 - \hat{\psi}_0$ .

*Proof of part (i).* We observe that,

$$\begin{aligned}\tau_{\hat{\mu}}^\mu \hat{\psi}_1 - \psi_1 &= \mathbb{P}_n \left[ \frac{AZ + AR}{\hat{\pi}(X)} - \left\{ \frac{A}{\hat{\pi}(X)} - 1 \right\} \{\tilde{m}_1(X) + D_1(X)\} \right] - \psi_1 \\ &= \underbrace{\mathbb{P}_n \left[ \frac{AZ}{\hat{\pi}(X)} - \left\{ \frac{A}{\hat{\pi}(X)} - 1 \right\} \tilde{m}_1(X) \right]}_{I_1} - \psi_1 + \underbrace{\mathbb{P}_n \left[ \frac{AR}{\hat{\pi}(X)} - \left\{ \frac{A}{\hat{\pi}(X)} - 1 \right\} D_1(X) \right]}_{II_1}.\end{aligned}$$

Consider the term  $II_1$ . It is seen that

$$\left\| \mathbb{P}_n \left[ \frac{AR}{\hat{\pi}(X)} \right] \right\|_\mu \leq \mathbb{P}_n \left\| \frac{AR}{\hat{\pi}(X)} \right\|_\mu \leq O(1) \mathbb{P}_n \|R\|_\mu = O_P(d(\hat{\mu}, \mu) + \alpha_n + \nu_n) = O_P(n^{-1/2}),$$

where we use the assumption that  $\hat{\pi}$  is uniformly bounded away from zero, the first equality is due to Lemma 7, and the last one is due to the assumptions on  $\alpha_n$  and  $\nu_n$  as well as Lemmas 9 and 10. For the second term in  $II_1$ ,

$$\left\| \mathbb{P}_n \left[ \left\{ \frac{A}{\hat{\pi}(X)} - 1 \right\} D_1(X) \right] \right\|_\mu \leq O(1) \mathbb{P}_n \|D_1(X)\|_\mu = O_P(d(\hat{\mu}, \mu) + \alpha_n + \nu_n) = O_P(n^{-1/2}),$$

where we use Assumptions 6(a) to obtain the first inequality, and Assumptions 4 or 9 to get the first equality. In summary,  $II_1 = O_P(n^{-1/2})$ .

For the term  $I_1$ , we have

$$\begin{aligned}I_1 &= \mathbb{P}_n \left[ \frac{A\{Z - \tilde{m}_1(X)\}}{\hat{\pi}(X)} + \tilde{m}_1(X) \right] - \psi_1 \\ &= (\mathbb{P}_n - \mathbb{E}_n) \left[ \frac{A\{Z - \tilde{m}_1(X)\}}{\hat{\pi}(X)} + \tilde{m}_1(X) \right] + \mathbb{E}_n \left[ \frac{A\{Z - \tilde{m}_1(X)\}}{\hat{\pi}(X)} + \tilde{m}_1(X) \right] - \psi_1 \\ &= (\mathbb{P}_n - \mathbb{E}_n) \left[ \frac{A\{Z - \tilde{m}_1(X)\}}{\hat{\pi}(X)} + \tilde{m}_1(X) - \frac{A\{Z - m_1^*(X)\}}{\pi^*(X)} - m_1^*(X) \right] \\ &\quad + (\mathbb{P}_n - \mathbb{E}_n) \left[ \frac{A\{Z - m_1^*(X)\}}{\pi^*(X)} + m_1^*(X) \right] + \mathbb{E}_n \left[ \frac{A\{Z - \tilde{m}_1(X)\}}{\hat{\pi}(X)} + \tilde{m}_1(X) \right] - \psi_1 \\ &= o_P(n^{-1/2}) + (\mathbb{P}_n - \mathbb{E}_n) \left[ \frac{A\{Z - m_1^*(X)\}}{\pi^*(X)} + m_1^*(X) \right] + \mathbb{E}_n \left[ \frac{A\{Z - \tilde{m}_1(X)\}}{\hat{\pi}(X)} + \tilde{m}_1(X) \right] - \mathbb{E}m_1(X) \\ &= o_P(n^{-1/2}) + \underbrace{(\mathbb{P}_n - \mathbb{E}_n) \left[ \frac{A\{Z - m_1^*(X)\}}{\pi^*(X)} + m_1^*(X) \right]}_{III_1} + \underbrace{\mathbb{E}_n \left[ \frac{\{\tilde{m}_1(X) - m_1(X)\}\{\hat{\pi}(X) - A\}}{\hat{\pi}(X)} \right]}_{IV_1},\end{aligned}\tag{S3}$$

where the SUTVA assumption is used in the last inequality. The forth equality above is due to Assumption 6(c)(d). Here,  $\mathbb{E}_n(O) = n^{-1} \sum_{i=1}^n \mathbb{E}(O_i)$  for generic random quantities  $O_1, \dots, O_n$ .

For the term  $\text{IV}_1$ , by Cauchy–Schwartz inequality, with Assumption 6(a), we have

$$\begin{aligned}
\text{IV}_1 &= \left\| \mathbb{E}_n \left[ \frac{\{\tilde{m}_1(X) - m_1(X)\}\{\hat{\pi}(X) - A\}}{\hat{\pi}(X)} \right] \right\|_{\mu} \\
&\leq c \left\| \mathbb{E}_n [\{\tilde{m}_1(X) - m_1(X)\}\{\hat{\pi}(X) - A\}] \right\|_{\mu} \\
&\leq c \mathbb{E}_n \left\| \{\tilde{m}_1(X) - m_1(X)\}\{\hat{\pi}(X) - \pi(X)\} \right\|_{\mu} + c \left\| \mathbb{E}_n [\{\tilde{m}_1(X) - m_1(X)\}\{\pi(X) - A\}] \right\|_{\mu} \\
&\leq cn^{-1} \sum_{i=1}^n \sqrt{\mathbb{E}\{|\hat{\pi}(X_i) - \pi(X_i)|^2\} \mathbb{E}\{\|\tilde{m}_1(X_i) - m_1(X_i)\|_{\mu}^2\}} + O(n^{-1/2} \varrho_m^{1/2}) \\
&= O(\varrho_{\pi} \varrho_m + n^{-1/2} \varrho_m + n^{-1/2} \varrho_{\pi}) + O(n^{-1/2} \varrho_m^{1/2}),
\end{aligned}$$

where  $c$  is a constant depending on the constant  $\epsilon$  in Assumption 6(a), and the last equality is obtained by using Assumption 6(b). In the above, the third inequality relies on the bound

$$\left\| \mathbb{E}_n [\{\tilde{m}_1(X) - m_1(X)\}\{\pi(X) - A\}] \right\|_{\mu} = O(n^{-1/2} \varrho_m^{1/2}), \quad (\text{S4})$$

which we establish below. Let  $V_i(g) = \{g(X_i) - m_1(X_i)\}\{\pi(X_i) - A_i\}$ ,  $\eta_i(g, h) = \|g(X_i) - h(X_i)\|_{\mu}$ ,  $\eta^2(g, h) = \frac{1}{n} \sum_{i=1}^n \eta_i^2(g, h)$ , and  $S_n(g) = \frac{1}{\sqrt{n}} \sum_{i=1}^n V_i(g)$ . Then  $S_n(m_1) = 0$ ,  $\mathbb{E}\{V_i(g)\} = 0$  and  $\mathbb{E}\{S_n(g)\} = 0$  for all  $m$ . In addition,  $\|V_i(g) - V_i(h)\|_{\mu} \leq |\pi(X_i) - A| \eta_i(g, h) \leq 2\eta_i(g, h)$ . Then, According to Assumption 6(e) and Theorem 6, holding  $\mathbb{X}$  fixed, we deduce that, for some universal constants  $c_0, b_0, r > 0$ ,

$$\text{pr} \left( \sup_{g \in B_r(m_1)} \frac{\|S_n(g)\|_{\mu}}{\eta(g, m_1)^{1/2}} \geq b\sqrt{K} \middle| \mathbb{X} \right) \leq \exp \left( - \frac{c_0 b K}{r} \right)$$

holds for all  $b \geq b_0$ . This further implies that

$$\mathbb{E} \left( \sup_{g \in B_r(m_1)} \frac{\|S_n(g)\|_{\mu}}{\eta(g, m_1)^{1/2}} \middle| \mathbb{X} \right) \leq c_1$$

for a fixed constant  $c_1$  for all  $\mathbb{X}$ , and further,  $\mathbb{E}(\|S_n(g)\|_{\mu} | \mathbb{X}) \leq c_1 \eta(g, m_1)^{1/2}$  for all  $g \in B_r(m_1)$ . By assumption,  $\tilde{m}_1 \in B_r(m_1)$  almost surely, and thus  $\mathbb{E}(\|S_n(\tilde{m}_1)\|_{\mu} | \mathbb{X}) \leq c_1 \eta(\tilde{m}_1, m_1)^{1/2}$ . Consequently,

$$\begin{aligned}
\left\| \mathbb{E}_n [\{\tilde{m}_1(X) - m_1(X)\}\{\pi(X) - A\}] \right\|_{\mu} &= n^{-1/2} \|\mathbb{E} S_n(\tilde{m}_1)\|_{\mu} \leq n^{-1/2} \mathbb{E}(\|S_n(\tilde{m}_1)\|_{\mu}) \\
&\leq c_1 n^{-1/2} \mathbb{E} \eta(\tilde{m}_1, m_1)^{1/2} \leq c_1 n^{-1/2} \{\mathbb{E} \eta^2(\tilde{m}_1, m_1)\}^{1/4}
\end{aligned}$$

$$= O(n^{-1/2} \varrho_m^{1/2}).$$

By a central limit theorem, we can conclude that  $\text{III}_1 = O_P(n^{-1/2})$ . Collecting all terms together, we deduce that  $\|\tau_{\hat{\mu}}^\mu \hat{\psi}_1 - \psi_1\|_\mu = O_P(n^{-1/2} + \varrho_\pi \varrho_m + n^{-1/2} \varrho_m^{1/2} + n^{-1/2} \varrho_\pi)$ . Similar derivations lead to  $\|\tau_{\hat{\mu}}^\mu \hat{\psi}_0 - \psi_0\|_\mu = O_P(n^{-1/2} + \varrho_\pi \varrho_m + n^{-1/2} \varrho_m^{1/2} + n^{-1/2} \varrho_\pi)$ . Then part (i) follows from  $\|\tau_{\hat{\mu}}^\mu \hat{\Delta}_{DR} - \Delta^\mu\|_\mu \leq \|\tau_{\hat{\mu}}^\mu \hat{\psi}_1 - \psi_1\|_\mu + \|\tau_{\hat{\mu}}^\mu \hat{\psi}_0 - \psi_0\|_\mu$ .  $\square$

*Proof of part (ii).* We start with a finer analysis on the term  $\text{II}_1$ , by first observing that

$$\mathbb{P}_n \left[ \left\{ \frac{A}{\hat{\pi}(X)} - 1 \right\} D_1(X) \right] = \mathbb{P}_n \left[ \left\{ \frac{A}{\pi(X)} - 1 \right\} D_1(X) \right] + \mathbb{P}_n \left[ \left\{ \frac{A\{\pi(X) - \hat{\pi}(X)\}}{\hat{\pi}(X)\pi(X)} \right\} D_1(X) \right].$$

In the above, the last term is of the order  $o_P(n^{-1/2})$  by Assumptions 2, 6(a)(c) and 4 on  $\pi, \hat{\pi}$  and  $D_1$ , along with the assumption  $\pi^* = \pi$  and Lemma 9. The term  $\mathbb{P}_n \left[ \left\{ \frac{A}{\pi(X)} - 1 \right\} D_1(X) \right]$  can be shown to have the order  $o_P(n^{-1/2})$  by an argument that is similar to the derivation of (S4).

For the first term in  $\text{II}_1$ , we observe that

$$\mathbb{P}_n \left[ \frac{AR}{\hat{\pi}(X)} \right] = \mathbb{P}_n \left[ \frac{AR}{\pi(X)} \right] + \mathbb{P}_n \left[ \frac{AR}{\hat{\pi}(X)} - \frac{AR}{\pi(X)} \right],$$

where the second term is dominated by the first one. Moreover,

$$\mathbb{P}_n \left[ \frac{AR}{\pi(X)} \right] = \mathbb{P}_n \left[ \frac{AU}{\pi(X)} \right] + \mathbb{P}_n \left[ \frac{AV}{\pi(X)} \right], \quad (\text{S5})$$

where  $U_i = \tau_{\hat{\mu}}^\mu \mathcal{L}_{\hat{\mu}} Y_i - \mathcal{L}_\mu Y_i$  and  $V_i = \tau_{\hat{\mu}}^\mu \mathcal{L}_{\hat{\mu}} \hat{Y}_i - \tau_{\hat{\mu}}^\mu \mathcal{L}_{\hat{\mu}} Y_i$ . By Lemma 8 and the assumptions on  $\alpha_n$  and  $\nu_n$ , we deduce that  $\mathbb{P}_n \left[ \frac{AV}{\pi(X)} \right] = o_P(n^{-1/2})$ .

For the first term in (S5), when  $\mathcal{M} = \mathcal{W}_2(\mathcal{I})$  and when  $\hat{\mu}$  is continuous,  $U_i = 0$ , and hence it is zero and further

$$\sqrt{n}(\tau_{\hat{\mu}}^\mu \hat{\psi}_1 - \psi_1) = \sqrt{n}(\mathbb{P}_n - \mathbb{E}) \left[ \frac{A\{Z - m_1^*(X)\}}{\pi^*(X)} + m_1^*(X) \right] + o_P(1), \quad (\text{S6})$$

since the assumptions on  $\varrho_m$  and  $\varrho_\pi$  gives rise to  $\text{IV}_1 = o(n^{-1/2})$ . Now we focus on the case that  $\mathcal{M}$  is a Riemannian manifold satisfying Assumption 5. Let  $\nabla$  be the covariant derivative, and define  $Q_i = -\nabla \mathcal{L}_\mu Y_i$ , which is a symmetric tensor defined in (5.3) of Kendall and Le (2011), and by the continuity and linearity of  $\nabla$ , satisfies  $\mathbb{E}\|Q_1\|^2 = O(1)$  uniformly around a neighborhood of  $\mu$ , given either the boundedness of  $\mathcal{M}$  or the Assumption 8. Then, by the first-order Taylor

series expansion at  $\mu$  (e.g., see the proof of Theorem 4 of Kendall and Le, 2011) and by the consistency of  $\hat{\mu}$  in Lemma 5,

$$\mathbb{P}_n \left[ \frac{AU}{\pi(X)} \right] = \mathbb{P}_n \left[ \frac{A(Q + \Xi)}{\pi(X)} \right] \mathcal{L}_\mu \hat{\mu} = \mathbb{P}_n \left[ \frac{AQ}{\pi(X)} \right] \mathcal{L}_\mu \hat{\mu} + o_P(\mathcal{L}_\mu \hat{\mu}) = \mathbb{P}_n \left[ \frac{AQ}{\pi(X)} \right] \mathcal{L}_\mu \hat{\mu} + o_P(n^{-1/2}),$$

where  $\Xi_i$  is as defined in the proof of Lemma 6 with  $y$  replaced by  $\hat{\mu}$ . In the above, the second equality is due to  $\mathbb{P}_n \Xi = o_P(1)$  established in the proof of Theorem 4 of Kendall and Le (2011), where we note that in the second condition of Theorem 4 of Kendall and Le (2011) the convergence can be weakened to a bound that decreases to zero as  $\rho \rightarrow 0$ , and in our application we can take  $\rho = n^{-1/3}$  since  $d(\hat{\mu}, \mu) = O_P(n^{-1/2}) \ll O_P(n^{-1/3})$ . By central limit theorem we conclude that  $\mathbb{P}_n \left[ \frac{AQ}{\pi(X)} \right] = \mathbb{E} \left[ \frac{AQ}{\pi(X)} \right] + o_P(n^{-1/2})$ . Let  $\mathcal{Q}_1$  denote  $\mathbb{E} \left[ \frac{AQ}{\pi(X)} \right]$ . Note that when the curvature is zero,  $\mathcal{Q}_1$  is an identity operator. In summary, we have showed that

$$\Pi_1 = \mathcal{Q}_1 \mathcal{L}_\mu \hat{\mu} + o_P(n^{-1/2}). \quad (\text{S7})$$

Recall that  $\tilde{\mu}$  is the empirical Fréchet mean of  $Y_1, \dots, Y_n$ . Using the fact that  $d(\hat{\mu}, \mu) = o_P(1)$  and  $d(\tilde{\mu}, \mu) = o_P(1)$  and Lemma 4 of Sun et al. (2019), we have  $\mathcal{L}_\mu \hat{\mu} = \mathcal{L}_\mu \tilde{\mu} + O_P(d(\hat{\mu}, \tilde{\mu})) = \mathcal{L}_\mu \tilde{\mu} + o_P(n^{-1/2})$ , where the last equality follows from Lemma 10 and the assumption on  $\alpha_n$ . Therefore,

$$\mathcal{Q}_1 \mathcal{L}_\mu \hat{\mu} = \mathcal{Q}_1 \mathcal{L}_\mu \tilde{\mu} + o_P(n^{-1/2}). \quad (\text{S8})$$

Let  $\mathcal{H}$  denotes the limit of  $\sum_{i=1}^n Q_i / \sum_{i=1}^n d^2(\mu, Y_i)$ ; the existence of the limit is established by Eq. (5.12) of Kendall and Le (2011). Now, by Eq. (5.10) of Kendall and Le (2011) and the proof therein, we have

$$\mathcal{L}_\mu \tilde{\mu} = (\mathcal{H} + o_P(1)) n^{-1} \sum_{i=1}^n \mathcal{L}_\mu Y_i = n^{-1} \sum_{i=1}^n \mathcal{H} \mathcal{L}_\mu Y_i + o_P(n^{-1/2}),$$

where the last equality is due to  $n^{-1} \sum_{i=1}^n \mathcal{L}_\mu Y_i = O_P(n^{-1/2})$  by a central limit theorem. Combining the above equation with (S3), (S7) and (S8), we conclude that

$$\sqrt{n}(\tau_\mu^\mu \hat{\psi}_1 - \psi_1) = \sqrt{n}(\mathbb{P}_n - \mathbb{E}) \left[ \frac{A\{Z - m_1^*(X)\}}{\pi^*(X)} + m_1^*(X) + \mathcal{Q}_1 \mathcal{H} Z \right] + o_P(1). \quad (\text{S9})$$

Similar deviations for the case  $a = 0$  lead to

$$\sqrt{n}(\tau_{\hat{\mu}}^\mu \hat{\psi}_1 - \psi_1) = \sqrt{n}(\mathbb{P}_n - \mathbb{E}) \left[ \frac{(1 - A)\{Z - m_0^*(X)\}}{1 - \pi^*(X)} + m_0^*(X) \right] + o_P(1) \quad (\text{S10})$$

when  $\mathcal{M} = \mathcal{W}_2(\mathcal{I})$ , and

$$\sqrt{n}(\tau_{\hat{\mu}}^\mu \hat{\psi}_1 - \psi_1) = \sqrt{n}(\mathbb{P}_n - \mathbb{E}) \left[ \frac{(1 - A)\{Z - m_0^*(X)\}}{1 - \pi^*(X)} + m_0^*(X) + \mathcal{Q}_0 \mathcal{H}Z \right] + o_P(1) \quad (\text{S11})$$

when  $\mathcal{M}$  is a Riemannian manifold satisfying Assumption 5, where  $\mathcal{Q}_0 = \mathbb{E} \left[ \frac{(1 - A)Q}{1 - \pi(X)} \right]$ .

Finally, by combining Equations (S6) and (S10) for the case  $\mathcal{M} = \mathcal{W}_2(\mathcal{I})$  and Equations (S9) and (S11) for the manifold case, the asymptotic normality of  $\tau_{\hat{\mu}}^\mu \hat{\Delta}_{DR}^{\hat{\mu}} - \Delta^\mu$  follows from a central limit theorem and Slutsky's lemma. Note that when the curvature is zero, we have  $\mathcal{Q}_1 = \mathcal{Q}_0$ . Then, both  $\mathcal{Q}_1$  and  $\mathcal{Q}_0$  vanish from the asymptotic normality of  $\tau_{\hat{\mu}}^\mu \hat{\Delta}_{DR}^{\hat{\mu}} - \Delta^\mu$ .  $\square$

## 4 Technical Lemmas

**Lemma 1.** For  $G_1, G_2, G \in \mathcal{W}_2(\mathcal{I})$ , we have  $\|\mathcal{L}_G G_1 - \mathcal{L}_G G_2\|_G = W_2(G_1, G_2)$ .

*Proof of Lemma 1.* The claims follows from the following observations:  $\|\mathcal{L}_G G_1 - \mathcal{L}_G G_2\|_G^2 = \int_{\mathcal{I}} |G_1^{-1} \circ G - G_2^{-1} \circ G|^2 dG = \int_0^1 |G_1^{-1}(t) - G_2^{-1}|^2 dt = W_2^2(G_1, G_2)$ , where the last equality is due to Theorem 2.18 of Villani (2003).  $\square$

**Lemma 2.** For a random element  $W$  on  $\mathcal{W}_2(\mathcal{I})$ ,  $\mathbb{E}W^{-1} = (\mathbb{E}W)^{-1}$  and  $\mathbb{E}\mathcal{L}_y W = \mathcal{L}_y \mathbb{E}W$  for any  $y \in \mathcal{W}_2(\mathcal{I})$ .

*Proof of Lemma 2.* The first assertion is a direct consequence of the isometry between  $\mathcal{W}_2(\mathcal{I})$  and the collection of quantile functions, viewed as a subspace of space  $L^2(\mathcal{I}; \lambda)$  of squared integrable functions endowed with the  $L^2$  distance  $\|f - g\| := \sqrt{\int_{\mathcal{I}} |f(x) - g(x)|_2^2 dx}$  (Theorem 2.18, Villani, 2003), where  $\lambda$  denotes the Lebesgue measure on  $\mathcal{I}$ .

For the second assertion,  $\mathbb{E}\mathcal{L}_y W = \mathbb{E}(W^{-1} \circ y) = (\mathbb{E}W^{-1}) \circ y = (\mathbb{E}W)^{-1} \circ y = \mathcal{L}_y \mathbb{E}W$ , where the third equality is due to the first assertion.  $\square$

**Lemma 3.** For the Fréchet function  $F(\cdot) = \mathbb{E}W_2^2(y, Y)$  of a random element  $Y$  on a Wasserstein space  $\mathcal{W}_2(\mathcal{I})$ , we have  $F(y) - F(\mu) = W_2^2(y, \mu)$  for all  $y \in \mathcal{W}_2(\mathcal{I})$ , where  $\mu$  is the Fréchet mean of  $Y$ .

*Proof of Lemma 3.* Let  $\langle g, h \rangle = \int_{\mathcal{I}} g(t)h(t)dt$  for two functions  $g$  and  $h$ . We first observe that

$$\begin{aligned} F(y) - F(\mu) &= \mathbb{E}W_2^2(y, Y) - \mathbb{E}d^2(\mu, Y) \\ &= \mathbb{E}(\langle y^{-1} - Y^{-1}, y^{-1} - Y^{-1} \rangle - \langle \mu^{-1} - Y^{-1}, \mu^{-1} - Y^{-1} \rangle) \\ &= \langle y^{-1} - \mu^{-1}, y^{-1} - \mu^{-1} \rangle - 2\mathbb{E}\langle y^{-1} - \mu^{-1}, \mu^{-1} - Y^{-1} \rangle \end{aligned}$$

$$\begin{aligned}
&= W_2^2(y, \mu) - 2\langle y^{-1} - \mu^{-1}, \mu^{-1} - \mathbb{E}Y^{-1} \rangle \\
&= W_2^2(y, \mu)
\end{aligned}$$

where the second equality is due to the isometry between  $\mathcal{W}_2(\mathcal{I})$  and the collection of quantile functions (Theorem 2.18, Villani, 2003), and the last equality is due to  $\mathbb{E}Y^{-1} = \mu^{-1}$  shown in Lemma 2.  $\square$

**Lemma 4.** *For Riemannian manifolds satisfying Assumption 5, the Riemannian logarithmic map  $\mathcal{L}_y \lambda$  is well defined for all  $y, \lambda \in \mathcal{M}$ . In addition, under Assumptions 5, the sample Fréchet mean  $\hat{\mu}$  of  $Y_1, \dots, Y_n \in \mathcal{M}$  exist and is unique. If in addition  $\mathbb{E}d^2(y, Y) < \infty$  for some  $y \in \mathcal{M}$ , then the population Fréchet mean  $\mu$  exists and is unique. Moreover,  $\hat{\mu}$  is the unique point in  $\mathcal{M}$  that satisfies  $\frac{1}{n} \sum_{i=1}^n \mathcal{L}_{\hat{\mu}}(Y_i) = 0$ , and  $\mu$  is the unique point in  $\mathcal{M}$  that satisfies  $\mathbb{E}\mathcal{L}_\mu Y = 0$ .*

*Proof of Lemma 4.* First, it is seen that the logarithmic map  $\mathcal{L}_y \lambda$  is well defined if there exists a unique minimizing geodesic connecting  $Y$  and  $\lambda$ . If  $\mathcal{M}$  is a Hadamard manifold, then it is uniquely geodesic, i.e., every two points are connected by a unique minimizing geodesic. If  $\mathcal{M}$  satisfies Assumption 5(b), then it is also uniquely geodesic according to Proposition 9.1.17 of Burago et al. (2001) combined with Theorem 1A.6 of Bridson and Häfliger (1999).

Either the boundedness of  $\mathcal{M}$  or Assumption 8 implies that  $\mathbb{E}d^2(p, Y) < \infty$  for some  $p \in \mathcal{M}$ , and further by triangle inequality, implies that the Fréchet function  $F(\cdot) = \mathbb{E}d^2(\cdot, Y)$  is finite everywhere. Corollary 2.1 of Alimisis et al. (2020) implies that  $F$  is strongly convex on  $\mathcal{M}$ . In addition, the continuity of the distance function implies the continuity of  $F$ . Then the Fréchet mean  $\mu$  exists and is unique according to Proposition 1.7 of Sturm (2003).

According to Theorem 2.1 of Bhattacharya and Patrangenaru (2003),  $\mu$  satisfies  $\mathbb{E}\mathcal{L}_\mu Y = 0$ . To see that  $\mu$  is the unique point in  $\mathcal{M}$  having this property, we first observe that the strong convexity of  $F$  implies that  $F$  has no local minimizer in  $\mathcal{M}$  other than  $\mu$ . When  $\mathcal{M}$  is characterized by Assumption 5(a), then the Hessian of  $h_p(y) = d^2(p, y)$  is positive everywhere according to the calculation in the proof of Lemma 12.15 of Lee (2018). When  $\mathcal{M}$  is characterized by Assumption 5(b), the Hessian comparison theorem (Theorem 11.7, Lee, 2018) together with the Hessian of spheres computed in Pennec (2018) implies that the Hessian of  $h_p(\cdot)$  is also positive on  $\mathcal{M}$ . Therefore,  $F$  has no stationary point in  $\mathcal{M}$ , and thus  $\mu$  is the only point in  $\mathcal{M}$  satisfies the first-order equation  $\mathbb{E}\mathcal{L}_\mu Y = 0$ . The same arguments apply to the empirical Fréchet mean.  $\square$

**Lemma 5.** *Suppose that  $\hat{\mu}$  is the empirical Fréchet mean of  $\widehat{Y}_1, \dots, \widehat{Y}_n$ , and  $\tilde{\mu}$  is the empirical Fréchet mean of  $Y_1, \dots, Y_n$  residing on  $\mathcal{M}$ . If  $\mathcal{M} = \mathcal{W}_2(\mathcal{I})$ , then we have  $d^2(\tilde{\mu}, \mu) = o_P(1)$ , and under additional Assumption 3 we have  $W_2^2(\hat{\mu}, \mu) = o_P(1)$ . If  $\mathcal{M}$  is a Riemannian manifold*

satisfying Assumption 5, then we have  $d^2(\tilde{\mu}, \mu) = o_P(1)$ , and under Assumption 7, we have  $d^2(\hat{\mu}, \mu) = o_P(1)$ .

*Proof of Lemma 5.* When  $\mathcal{M} = \mathcal{W}_2(\mathcal{I})$ , as in the proof of Lemma 3, according to the isometry between  $\mathcal{W}_2(\mathcal{I})$  and the collection of quantile functions (Theorem 2.18, Villani, 2003),  $W_2^2(\tilde{\mu}, \mu) = o_P(1)$  if and only if  $\|\tilde{\mu}^{-1} - \mu^{-1}\|_2 = o_P(1)$ , where  $\|g\|_2^2 = \int_{\mathcal{I}} |g(t)|^2 dt$  for any measurable function  $g$ . By Lemma 2,  $\tilde{\mu}^{-1} = n^{-1} \sum_{i=1}^n Y_i^{-1}$  and  $\mathbb{E} Y_i^{-1} = \mu^{-1}$ . Then  $\|\tilde{\mu}^{-1} - \mu^{-1}\|_2 = o_P(1)$  follows from the weak law of large numbers.

To prove  $W_2^2(\hat{\mu}, \mu) = o_P(1)$ , we apply Lemma 2 to the uniform distribution on the discrete set  $\{\hat{Y}_1, \dots, \hat{Y}_n\}$  and its Fréchet mean  $\hat{\mu}$ , and deduce  $\hat{\mu}^{-1} = (n^{-1} \sum_{i=1}^n \hat{Y}_i^{-1})$ . Similarly,  $\tilde{\mu}^{-1} = (n^{-1} \sum_{i=1}^n Y_i^{-1})$ . Then

$$\begin{aligned} W_2(\hat{\mu}, \tilde{\mu}) &= \|\hat{\mu}^{-1} - \tilde{\mu}^{-1}\|_2 = \left\| n^{-1} \sum_{i=1}^n \hat{Y}_i^{-1} - n^{-1} \sum_{i=1}^n Y_i^{-1} \right\|_2 \\ &\leq n^{-1} \sum_{i=1}^n \|\hat{Y}_i^{-1} - Y_i^{-1}\|_2 = n^{-1} \sum_{i=1}^n W_2(\hat{Y}_i, Y_i) = O_P(\alpha_n) = o_P(1), \end{aligned}$$

where the third equality is due to Assumption 3 and Markov's inequality. Then  $W_2(\hat{\mu}, \mu) \leq W_2(\hat{\mu}, \tilde{\mu}) + W_2(\tilde{\mu}, \mu) = o_P(1)$ .

When  $\mathcal{M}$  is a Riemannian manifold satisfying Assumption 5, we have  $d(\tilde{\mu}, \mu) = o_P(1)$  according to Theorem 2.3 of Bhattacharya and Patrangenaru (2003), and by slightly modifying the proof of the theorem, we can show that  $d(\hat{\mu}, \mu) = o_P(1)$  under the additional Assumption 7.  $\square$

The following result quantifies the average deviation between  $\mathcal{L}_{\hat{\mu}} Y_i$  and  $\mathcal{L}_{\mu} Y_i$  induced by the difference between  $\hat{\mu}$  and  $\mu$ .

**Lemma 6.** *For a Riemannian manifold  $\mathcal{M}$  satisfying Assumption 5, for the Fréchet mean  $\mu$  of  $Y_1$  residing on  $\mathcal{M}$ , for any fixed  $\epsilon > 0$ , for any  $\lambda \in \mathcal{M}$  such that  $d(\lambda, \mu) < \epsilon$ , we have*

$$\frac{1}{n} \sum_{i=1}^n \|\tau_{\lambda}^{\mu} \mathcal{L}_{\lambda} Y_i - \mathcal{L}_{\mu} Y_i\|_{\mu}^2 = O_P(d^2(\lambda, \mu)). \quad (\text{S12})$$

*Proof of Lemma 6.* To simplify notation, write  $\tilde{V}_i = \mathcal{L}_{\lambda} Y_i$  and  $V_i = \mathcal{L}_{\mu} Y_i$ . As in the proof of Theorem 4 of Kendall and Le (2011), we have

$$\tau_{\lambda}^{\mu} \tilde{V}_i = V_i + \nabla_{\mathcal{L}_{\mu} \lambda} V_i + \Xi_i \mathcal{L}_{\mu} \lambda,$$

where  $\Xi_i U = \sum_{r=1}^q \tau_y^{\mu} \nabla_U Z_{r,i}(y) - \nabla_U Z_{r,i}(\mu)$  for  $Z_{r,i}(y) = g_y(\mathcal{L}_y Y_i, e_r) e_r$ ,  $e_1, \dots, e_q$  denote an orthonormal frame in  $B_{\epsilon}(\mu) = \{q \in \mathcal{M} : d(q, \mu) < \epsilon\}$ ,  $q$  denotes the dimension of  $\mathcal{M}$ , and  $y$  lies

in the geodesic connecting  $\mu$  and  $\lambda$ . As  $\nabla$  is continuous in a local unit bundle on  $B_\epsilon(\mu)$ , with probability tending to one,

$$\|\tau_\lambda^\mu \tilde{V}_i - V_i\|_\mu^2 \leq K_1 \|\mathcal{L}_\mu \lambda\|_\mu^2 \|V_i\|_\mu^2 + K_2 \|\mathcal{L}_\mu \lambda\|_\mu^2 \|V_i\|_\mu^2$$

for some constants  $K_1, K_2$  depending only on  $\epsilon, \mu$  and  $\mathcal{M}$ , where we use the bound  $\|\mathcal{L}_y Y_i\|_y = d(y, Y_i) \leq d(y, \mu) + d(\mu, Y_i) \leq d(\lambda, \mu) + d(\mu, Y_i) = \|\mathcal{L}_\mu \lambda\|_\mu + \|V_i\|_\mu$ . Then the result follows from that  $n^{-1} \sum_{i=1}^n \|V_i\|_\mu \rightarrow \mathbb{E} \|V_1\|_\mu$  in probability by the weak law of large numbers and by either the boundedness of  $\mathcal{M}$  or the subgaussianity that implies  $\mathbb{E} \|V_1\|_\mu^2 < \infty$ .  $\square$

The following result, which is similar to Lemma 6, takes the additional error induced by the surrogate observations into account.

**Lemma 7.** *For the empirical Fréchet mean  $\hat{\mu}$  of  $\widehat{Y}_1, \dots, \widehat{Y}_n$ , if  $\mathcal{M} = \mathcal{W}_2(\mathcal{I})$  and  $\hat{\mu}$  is continuous, then under Assumption 3,*

$$\frac{1}{n} \sum_{i=1}^n \|\tau_{\hat{\mu}}^\mu \mathcal{L}_{\hat{\mu}} \widehat{Y}_i - \mathcal{L}_\mu Y_i\|_\mu^2 = O_P(\alpha_n^2 + \nu_n^2),$$

and if  $\mathcal{M}$  is a Riemannian manifold satisfying Assumption 5, then under Assumption 7,

$$\frac{1}{n} \sum_{i=1}^n \|\tau_{\hat{\mu}}^\mu \mathcal{L}_{\hat{\mu}} \widehat{Y}_i - \mathcal{L}_\mu Y_i\|_\mu^2 = O_P(d^2(\hat{\mu}, \mu) + \alpha_n^2 + \nu_n^2). \quad (\text{S13})$$

*Proof of Lemma 7.* Given the following observation

$$\frac{1}{n} \sum_{i=1}^n \|\tau_{\hat{\mu}}^\mu \mathcal{L}_{\hat{\mu}} \widehat{Y}_i - \mathcal{L}_\mu Y_i\|_\mu^2 \leq \frac{2}{n} \sum_{i=1}^n \|\tau_{\hat{\mu}}^\mu \mathcal{L}_{\hat{\mu}} Y_i - \mathcal{L}_\mu Y_i\|_\mu^2 + \frac{2}{n} \sum_{i=1}^n \|\tau_{\hat{\mu}}^\mu \mathcal{L}_{\hat{\mu}} \widehat{Y}_i - \tau_{\hat{\mu}}^\mu \mathcal{L}_{\hat{\mu}} Y_i\|_\mu^2,$$

for the case  $\mathcal{M} = \mathcal{W}_2(\mathcal{I})$  the conclusion is a direct consequence of Lemma 8 and the fact that  $\tau_{\hat{\mu}}^\mu \mathcal{L}_{\hat{\mu}} Y_i - \mathcal{L}_\mu Y_i = 0$  when  $\hat{\mu}$  is continuous (so that  $\hat{\mu} \circ \hat{\mu}^{-1} = \text{id}$ ), and for the case that  $\mathcal{M}$  is a manifold it is a consequence of Lemmas 6 and 8.  $\square$

**Lemma 8.** *Under Assumption 3 when  $\mathcal{M} = \mathcal{W}_2(\mathcal{I})$ , and under Assumption 7 when  $\mathcal{M}$  that is a Riemannian manifold satisfying Assumption 5, then for a fixed  $\epsilon > 0$ , we have*

$$\sup_{\lambda: d(\lambda, \mu) < \epsilon} \frac{1}{n} \sum_{i=1}^n \|\mathcal{L}_\lambda \widehat{Y}_i - \mathcal{L}_\lambda Y_i\|_\lambda^2 = O_P(\alpha_n^2 + \nu_n^2),$$

where  $d$  denotes the distance on the space  $\mathcal{M}$ .

*Proof of Lemma 8.* The case that  $\mathcal{M} = \mathcal{W}_2(\mathcal{I})$  follows from Lemma 1 and Assumption 3. When  $\mathcal{M}$  is a Riemannian manifold satisfying Assumption 5, using Lemma 4 of Sun et al. (2019), we deduce that

$$\begin{aligned} \frac{1}{n} \sum_{i=1}^n \|\mathcal{L}_\lambda \widehat{Y}_i - \mathcal{L}_\lambda Y_i\|_\lambda^2 &\leq \frac{1}{n} \sum_{i=1}^n (1 + c_0 H_i^2)^2 d^2(\widehat{Y}_i, Y_i) \\ &\leq \sqrt{\frac{1}{n} \sum_{i=1}^n (1 + c_0 H_i^2)^4} \sqrt{\frac{1}{n} \sum_{i=1}^n d^4(\widehat{Y}_i, Y_i)} \\ &\leq c_1 \sqrt{1 + \frac{c_0^4}{n} \sum_{i=1}^n H_i^8} \sqrt{\frac{1}{n} \sum_{i=1}^n d^4(\widehat{Y}_i, Y_i)} \end{aligned} \quad (\text{S14})$$

where  $H_i = \max\{d(\lambda, \widehat{Y}_i), d(\lambda, Y_i)\} \leq \max\{d(\lambda, \widehat{Y}_i), d(\lambda, Y_i)\} + d(\lambda, \mu)$ ,  $c_0 > 0$  is a constant depending on the curvature of the manifold  $\mathcal{M}$ , and  $c_1 > 0$  is an absolute constant. Then,

$$\begin{aligned} \frac{1}{n} \sum_{i=1}^n H_i^8 &\leq c_2 d^8(\lambda, \mu) + \frac{c_2}{n} \sum_{i=1}^n (\max\{d(\lambda, \widehat{Y}_i), d(\lambda, Y_i)\})^8 \\ &\leq c_2 d^8(\lambda, \mu) + \frac{c_3}{n} \sum_{i=1}^n \{d^8(\lambda, \widehat{Y}_i) + d^8(\lambda, Y_i)\} \\ &= O_P(1), \end{aligned}$$

where  $c_2, c_3 > 0$  are absolute constants, and we use either the boundedness of  $\mathcal{M}$  or the moment conditions in Assumption 8. The conclusion of the lemma follows from (S14) and Assumption 7 that implies

$$\mathbb{E} \left| \frac{1}{n} \sum_{i=1}^n d^4(\widehat{Y}_i, Y_i) \right| \leq \frac{1}{n} \sum_{i=1}^n \mathbb{E} d^4(\widehat{Y}_i, Y_i) = \alpha_n^4 + \nu_n^4,$$

which further suggests that  $\frac{1}{n} \sum_{i=1}^n d^4(\widehat{Y}_i, Y_i) = O_P(\alpha_n^4 + \nu_n^4)$ .  $\square$

**Lemma 9.** Suppose that  $\hat{\mu}$  is the empirical Fréchet mean of  $\widehat{Y}_1, \dots, \widehat{Y}_n \in \mathcal{W}_2(\mathcal{I})$ , and  $\tilde{\mu}$  is the empirical Fréchet mean of  $Y_1, \dots, Y_n \in \mathcal{W}_2(\mathcal{I})$ . Then, we have  $W_2^2(\tilde{\mu}, \mu) = O_P(n^{-1})$ . Suppose further that Assumption 3 holds, then we have  $W_2^2(\hat{\mu}, \tilde{\mu}) = O_P(\alpha_n^2)$  and  $W_2^2(\hat{\mu}, \mu) = O_P(n^{-1} + \alpha_n^2)$ .

The following result is in analogy to Lemma 9 that establishes the convergence rate of the empirical Fréchet means. Note that, although the properties of the empirical Fréchet mean  $\hat{\mu}$  have been studied in the literature (Bhattacharya and Patrangenaru, 2003, 2005; Schötz, 2019), none of them considers its properties when the observations are not fully observed.

**Lemma 10.** Suppose that  $\hat{\mu}$  is the empirical Fréchet mean of  $\widehat{Y}_1, \dots, \widehat{Y}_n$ , and  $\tilde{\mu}$  is the empirical Fréchet mean of  $Y_1, \dots, Y_n$  residing on a Riemannian manifold  $\mathcal{M}$  that satisfies Assumption 5. In addition, suppose that  $\mathbb{E}d^2(p, Y) < \infty$  for some  $p \in \mathcal{M}$  if  $\mathcal{M}$  is a manifold characterized by Assumption 5(a). We have  $d^2(\tilde{\mu}, \mu) = O_P(n^{-1})$ . Under Assumption 7, we have  $d^2(\hat{\mu}, \mu) = O_P(n^{-1} + \alpha_n^2)$  and  $d^2(\hat{\mu}, \tilde{\mu}) = O_P(\alpha_n^2)$ .

*Proof of Lemmas 9 and 10.* We apply the general theory from Schötz (2019). According to the discussion in Section 3 of Schötz (2019), the weak quadruple condition holds for a Wasserstein space  $\mathcal{W}_2(\mathcal{I})$  or a manifold satisfying Assumption 5. The moment condition is either assumed or given by the boundedness of  $\mathcal{W}_2(\mathcal{I})$  and  $\mathcal{M}$ . In light of Lemma 5 and according to Schötz (2019), it is sufficient to verify the entropy condition and the growth condition in a neighborhood of  $\mu$ .

The growth condition for the Wasserstein space  $\mathcal{W}_2(\mathcal{I})$  is verified in Lemma 3. For a manifold satisfying Assumption 5, Corollary 2.1 of Alimisis et al. (2020) and Theorem 2.1 of Bhattacharya and Patrangenaru (2003) together imply the growth condition of Schötz (2019).

We now verify the entropy condition of Schötz (2019). If  $\mathcal{M} = \mathcal{W}_2(\mathcal{I})$ , then the entropy condition holds as  $\sup_{\omega \in \mathcal{W}_2(\mathcal{I})} \log N(\delta\epsilon, B_\delta(\omega), d) \leq K\epsilon^{-1}$  shown in the proof of Proposition 1 of Petersen and Müller (2019). When  $\mathcal{M}$  is a manifold, if it is compact, then its curvature is bounded away from  $-\infty$  and  $+\infty$ . According to the Bishop–Günther inequality (Gray, 2004, Eq. (3.34)),  $\text{vol}(B_\epsilon(\lambda)) \geq C_1\epsilon^D$  for all sufficiently small  $\epsilon > 0$ , where  $D$  is the dimension of  $\mathcal{M}$ ,  $B_\epsilon(\lambda) = \{y \in \mathcal{M} : d(y, \lambda) < \epsilon\}$  and  $C_1$  is a constant independent of  $\lambda$  and  $\epsilon$ . With this result and equation (3.33) of Gray (2004), the packing number and thus the covering number of  $B_\delta(\mu)$  is bounded by  $O(\delta^D\epsilon^{-D})$ . Therefore, the entropy condition holds for  $\alpha = \beta = 1/2$  for a sufficiently small neighborhood of  $\mu$ . Then the conclusion  $d^2(\tilde{\mu}, \mu) = O_P(n^{-1})$  follows directly from Corollary 1 of Schötz (2019).

Now we modify the proof for Theorem 1 of Schötz (2019) to the case that only noisy surrogates  $\widehat{Y}_1, \dots, \widehat{Y}_n$  are observable. Let  $\tilde{F}_n(y) = n^{-1} \sum_{i=1}^n d^2(y, Y_i)$  and  $F_n(y) = n^{-1} \sum_{i=1}^n d^2(y, \widehat{Y}_i)$ . Define

$$\begin{aligned}\tilde{\Xi}_n(\delta) &:= \sup_{y \in \mathcal{M}: d(y, \mu) < \delta} \tilde{F}(y) - \tilde{F}(\mu) - \tilde{F}_n(y) + \tilde{F}_n(\mu), \\ \Xi_n(\delta) &:= \sup_{y \in \mathcal{M}: d(y, \mu) < \delta} \tilde{F}(y) - \tilde{F}(\mu) - F_n(y) + F_n(\mu).\end{aligned}$$

According to Lemma 2 of Schötz (2019), we just need to show that  $\mathbb{E}\{\Xi_n^2(\delta)\} \leq c_1(n^{-1} + \alpha_n^2)\delta^2$

for some constant  $c_1 > 0$  and all  $\delta > 0$ . First, we observe that  $\Xi_n(\delta) \leq \tilde{\Xi}_n(\delta) + G_n(\delta)$ , where

$$\begin{aligned} G_n(\delta) &= \sup_{y \in \mathcal{M}: d(y, \mu) < \delta} \frac{1}{n} \sum_{i=1}^n \{d^2(y, \widehat{Y}_i) - d^2(y, Y_i) - d^2(\mu, \widehat{Y}_i) + d^2(\mu, Y_i)\} \\ &\leq \sup_{y \in \mathcal{M}: d(y, \mu) < \delta} \frac{1}{n} \sum_{i=1}^n d(y, \mu) d(Y_i, \widehat{Y}_i) \leq \delta \frac{1}{n} \sum_{i=1}^n d(Y_i, \widehat{Y}_i), \end{aligned}$$

where the first inequality is due to the Weak Quadruple condition; see Section 3.2.3 of Schötz (2019) for details. Thus, according to Assumption 3 or 7,

$$\mathbb{E}\{G_n^2(\delta)\} \leq \delta^2 \mathbb{E} \left\{ \frac{1}{n} \sum_{i=1}^n d(Y_i, \widehat{Y}_i) \right\}^2 \leq \delta^2 \frac{1}{n} \sum_{i=1}^n \mathbb{E} d^2(Y_i, \widehat{Y}_i) \leq \delta^2 \alpha_n^2.$$

According to Lemma 3 of Schötz (2019), we have  $\mathbb{E}\{\tilde{\Xi}_n^2(\delta)\} \leq c_2 \delta^2/n$  for some constant  $c_2 > 0$ . Consequently,

$$\mathbb{E}\{\Xi_n^2(\delta)\} \leq 2\mathbb{E}\{\tilde{\Xi}_n^2(\delta)\} + 2\mathbb{E}\{G_n^2(\delta)\} \leq 2(c_2 + 1)(n^{-1} + \alpha_n^2)\delta^2.$$

The proof for  $d^2(\hat{\mu}, \mu)$  is completed by setting  $c_1 = 2(c_2 + 1)$ . The result for  $d^2(\hat{\mu}, \tilde{\mu})$  follows from the same line of argument, conditional on  $Y_1, \dots, Y_n$ .  $\square$

## 5 Function-valued Empirical Processes

In the proof of Theorems 3 and 5 we came cross the problem of finding the convergence rate of a random quantity in the form  $n^{-1/2} \sum_{i=1}^n h(\xi_i) \{\hat{g}(\xi_i) - g_0(\xi_i)\}$  for fixed functions  $h, g_0$  and independent observations  $\xi_1, \dots, \xi_n$  such that  $\mathbb{E}h(\xi_i)g(\xi_i) = 0$  for any  $g$ ; here  $\hat{g}$  is an estimate for  $g_0$  based on  $\xi_1, \dots, \xi_n$  (and potentially on some other fixed quantities). For example,  $\xi_i = A_i$ ,  $h(\xi_i) = \pi(X_i) - A_i$ ,  $g_0 = m_a$ , and  $\hat{g} = \tilde{m}_a$  in the proof of (S4), where we hold  $X_i$  fixed. Such problem is also encountered in other scenarios of statistical research, for instance, in the proof of Theorem 9 of Mammen and van de Geer (1997). Unique in our context is that the function  $\hat{g}$  may take values in a space of functions, e.g., in the case of  $\mathcal{W}_2(\mathcal{I})$ , so that the classic results in van de Geer (1990) do not apply directly and need to be extended. Instead of function spaces, below we consider more generally a separable Hilbert space that includes some function spaces as special examples.

To set the stage, let  $\mathcal{X}$  be a compact space and  $\nu$  a positive measure on it. Suppose that  $\mathcal{H}$  is a separable Hilbert space, and  $\mathcal{F}$  is a class of functions that maps  $\mathcal{X}$  into  $\mathcal{H}$ . An immediate example of  $\mathcal{H}$  is the space  $L^2([0, 1])$  of real-valued squared integrable function defined on

$[0, 1]$ . Consider an  $\mathcal{H}$ -valued random process  $S_n$  indexed by  $\mathcal{F}$  of the form

$$S_n(g) = \frac{1}{\sqrt{n}} \sum_{i=1}^n V_i(g),$$

where  $V_1, \dots, V_n$  are independent  $\mathcal{H}$ -valued centered random process defined on  $\mathcal{F}$ . For instance, in the above context,  $V_i(g) = h(\xi_i)\{g(\xi_i) - g_0(\xi_i)\}$  for each  $g \in \mathcal{F}$ .

Let  $\eta$  be a pseudo-distance on  $\mathcal{F}$  of the form  $\eta^2(f, g) = n^{-1} \sum_{i=1}^n \eta_i^2(f, g)$ , where  $\eta_1, \dots, \eta_n$  are also pseudo-distance on  $\mathcal{F}$ , e.g.,  $\eta_i(g_1, g_2) = \|g_1(\xi_i) - g_2(\xi_i)\|_{\mathcal{H}}$  with  $\|\cdot\|_{\mathcal{H}}$  denoting the norm on the Hilbert space  $\mathcal{H}$ . Suppose  $S_n(g_0) = 0$  for  $g_0 \in \mathcal{F}$  and  $\|V_i(g_1) - V_i(g_2)\|_{\mathcal{H}} \leq M_i \eta_i(g_1, g_2)$ , where  $M_1, \dots, M_n$  are uniformly subgaussian random variables, i.e,

$$\sup_i \mathbb{E} \exp\{\beta^2 M_i^2\} \leq \Gamma < 0 \quad (\text{S15})$$

for some absolute constants  $\beta, \Gamma > 0$ . Finally, let  $\mathcal{K}(\delta, r)$  be the local entropy of a ball  $B(r; g_0) \subset \mathcal{F}$  with respect to the pseudo-distance  $\eta$ . Without loss of generality we assume  $\mathcal{K}$  is continuous in  $\delta$ ; otherwise, we just define it to be a continuous function that upper bounds the local entropy.

**Theorem 6.** *Suppose (S15) holds and  $\mathcal{K}(\delta, r) \leq K\delta^{-2\zeta}$  for some  $K > 0$  and  $\zeta \in (0, 1)$ . Then, there exist constants  $b_0$  and  $c$ , depending only on  $\beta$  and  $\Gamma$ , such that for any  $b \geq b_0$ , we have*

$$\text{pr} \left( \sup_{g \in B(r; g_0)} \frac{\|S_n(g)\|_{\mathcal{H}}}{\{\eta(g, g_0)\}^{1-\zeta}} \geq b\sqrt{K} \right) \leq \exp\left(-\frac{cb^2K}{r^{2\zeta}}\right) \quad (\text{S16})$$

for all  $n \geq 1$ .

*Proof.* The subgaussian assumption implies that Eq (3.10) of Kuelbs (1978) is valid for  $S_n(g_1 - g_2)$  for all  $g_1, g_2 \in \mathcal{F}$ . Then, (S16) follows from the argument that leads to Lemma 3.5 of van de Geer (1990).  $\square$

## 6 The Log-Cholesky Metric for SPD Matrices

When equipped with the log-Cholesky metric (Lin, 2019),  $\text{Sym}^+(3)$  becomes a Riemannian manifold of zero curvature. To describe such metric, we first recall that every  $Q \in \text{Sym}^+(3)$  admits the Cholesky decomposition  $Q = LL^\top$  for a lower triangular matrix  $L$ , and such decomposition is unique if we require the diagonal elements of  $L$  to be positive. This unique  $L$  is called the Cholesky factor of  $Q$ . For  $S \in \text{Sym}(3)$ , we use  $S_{1/2}$  to denote the lower triangular matrix

whose strictly lower triangular part is equal to the strictly lower triangular part of  $S$  and whose diagonal elements are the diagonal elements of  $S/2$ . To define the Riemannian metric at  $Q \in \text{Sym}^+(3)$  whose Cholesky factor is  $L$ , for  $S \in \text{Sym}(3)$  we write  $h_S = L\{L^{-1}S(L^{-1})^\top\}_{1/2}$  which is a lower triangular matrix. Then the Riemannian metric  $g_Q$  at  $Q \in \text{Sym}^+(3)$  is  $g_Q(R, S) = \sum_{j>k} h_R(j, k)h_S(j, k) + \sum_{j=1}^3 h_R(j, j)h_S(j, j)\{L(j, j)\}^{-2}$ , where for a general matrix  $V$ ,  $V(j, k)$  denotes the element at the  $j$ th row and  $k$ th column of  $V$ . If we write  $\Phi_L(K) = [K + L] + \mathbb{D}(L)\exp\{\mathbb{D}(K)\mathbb{D}(L)^{-1}\}$  and  $\Psi_L(K) = [K - L] + \mathbb{D}(L)\log\{\mathbb{D}(K)\mathbb{D}(L)^{-1}\}$ , where  $[K]$  denotes the strictly lower triangular part of  $K$ ,  $\mathbb{D}(K)$  denotes the diagonal part of  $K$ , and  $\exp(D)$  (resp.  $\log(D)$ ) for a diagonal matrix is the matrix obtained by applying the real exponential function  $x \mapsto e^x$  (resp. the real logarithmic function  $x \mapsto \log x$ ) to each diagonal elements of  $D$ , then the Riemannian exponential map is given by  $\mathcal{E}_Q S = \Phi_L(h_S)\{\Phi_L(h_S)\}^\top$  for  $S \in \text{Sym}(3)$  and the Riemannian logarithmic map is given by  $\mathcal{L}_Q(V) = L\{\Psi_L(R)\}^\top + \Psi_L(R)L^\top$  for  $V \in \text{Sym}^+(3)$  with the Cholesky factor  $R$ .